



**Technische Universität Braunschweig**  
**Leichtweiß-Institute for Hydraulic Engineering and Water Resources**  
**Department of Hydromechanics and Coastal Engineering**

Prof. Dr.-Ing. Hocine Oumeraci

Report No. 002 (Draft)

## **Reliability Assessment of the Falster Dike in Denmark**

Prof. Dr.-Ing. H. Oumeraci  
Dr.-Ing. A. Kortenhaus  
D. Schürenkamp

Braunschweig, September 2012

## Contents

List of Figures .....	iii
List of Tables.....	v
Index of Notations and Symbols .....	vi
1 Introduction .....	7
1.1 Motivation and Objectives.....	7
1.2 Investigation Area.....	7
2 Data Processing and Boundary Conditions .....	8
2.1 Topography and Bathymetry .....	8
2.1.1 Topography of Dike and Dunes .....	8
2.1.2 Bathymetry.....	8
2.2 Hydraulic Boundary Conditions .....	9
2.2.1 Water Level and Storm Surge Scenarios .....	9
2.2.2 Wind Parameters .....	10
2.2.3 Sea State.....	10
2.3 Beach and Dune Erosion .....	11
3 Methodology .....	13
4 Results .....	14
4.1 Sea State Simulation with SWAN .....	14
4.2 Simulation of Beach and Dune Erosion.....	17
4.2.1 Numerical Model XBeach .....	17
4.2.2 Dune Erosion .....	17
4.2.3 Wave Runup and Overwash.....	19
4.2.4 Dune Crossing.....	21
4.2.5 Summary of Beach and Dune Erosion.....	21
4.3 Deterministic Analysis of Wave Loading.....	22
4.3.1 Assessment of Dike without Considering Dunes.....	22
4.3.2 Assessment of Dike with Berm.....	23
4.4 Probabilistic Analysis of Wave Loading .....	26
4.4.1 Assessment of Dike with Berm.....	26
4.4.2 Probability Calculation .....	26
5 Conclusions, Recommendations and Outlook .....	27

---

Literature .....	29
Appendix .....	30
Appendix A: Overview of Dike and Dune Sections.....	31
Appendix B: Determination of the Berm Factor .....	32
Appendix C: Results of Sea State Simulation (SWAN).....	34
Appendix D: Simulated Dune Erosion Cross Profiles.....	35
Appendix E: Runup Level for Each Scenario .....	38
Appendix F: Fault Tree of Probabilistic Approach.....	41

## List of Figures

Fig. 1.1: Investigation area with topography and bathymetry (Data source: DCA, 2011 and FDB, 2011)	7
Fig. 2.1: Detail of topography of Falster Dike with dunes - example of crossing no. 5 in Marielyst (Data source: FDB, 2011)	8
Fig. 2.2: Bathymetry of baltic sea at the Falster Island (Data source: DCA, 2011 and Seifert et al., 2001)	8
Fig. 2.3: Development of water level $h_w$ of four storm surge scenarios	9
Fig. 2.4: Maximum wind speed from directions $0^\circ - 180^\circ$	10
Fig. 3.1: Classification of coastal protection system	13
Fig. 4.1: Wave height $H_{sig}$ for each dike section in a distance of 100 m to the coastline	15
Fig. 4.2: Wave period $T_{m01}$ for each dike section in a distance of 100 m to the coastline	15
Fig. 4.3: Mean wave direction $\theta$ for each dike section in a distance of 100 m to the coastline	16
Fig. 4.4: $H_{sig}$ at the model boundary of the cross profile 9+000	16
Fig. 4.5: Initial and erosion profiles of each dune profile	18
Fig. 4.6: Wave runup and dune breach, 4 <sup>th</sup> erosion profile dune section DIII and scenario D	20
Fig. 4.7: Wave runup at crossing Marielyst (left) and Falster south end (without dike behind) (right)	21
Fig. 4.8: Dune with asphalt cover layer at crossing no. 5 in Marielyst	21
Fig. 4.9: Calculated maximum wave overtopping rates ordered by dike sections for each water level scenario with updated dike slopes [ $q_{max} = 6.1 \text{ l/(s}\cdot\text{m)}$ ]	23
Fig. 4.10: Determination of effective berm length and berm width (dune section DI) (Scenario D)	23
Fig. 4.11: Berm factor $\gamma_b$ for each dune section (Scenario A)	24
Fig. 4.12: Berm factor $\gamma_b$ for each dune section (Scenario B)	24
Fig. 4.13: Berm factor $\gamma_b$ for each dune section (Scenario C)	24
Fig. 4.14: Berm factor $\gamma_b$ for each dune section (Scenario D)	24

Fig. 4.15: Berm width $B$ for each dune section	25
Fig. 4.16: Berm height $h_B$ for each dune section	25
Fig. 4.17: Calculated maximum wave overtopping rates ordered by dike sections for each water level scenario with consideration of completely eroded dunes [ $q_{\max} = 0.5 \text{ l}/(\text{s}\cdot\text{m})$ ]	25
Fig. 4.18: Berm factor for each dune section (percentage rate of berm influence) (Scenario D)	26

## List of Tables

Tab. 2.1: Water level scenarios	9
Tab. 2.2: SWAN boundary conditions at offshore border	11
Tab. 2.3: Dune sections with stations marks	12
Tab. 4.1: Characteristics of the SWAN model grids	14
Tab. 4.2: Results of probability calculation	27

## Index of Notations and Symbols

DCA	Danish Coastal Authority (Kystdirektoratet)
DMI	Danish Meteorological Institute (Danmarks Meteorologiske Institut)
DVR	Danish Vertical Reference 1990
FDB	Falster Dike Board (Det falsterske digelag)
GIS	Geographic information system
LIDAR	Light detection and ranging
LWI	Leichtweiß-Institute for Hydraulic Engineering and Water Resources
B	Berm width [m]
g	Gravity [ $m/s^2$ ]
h	Water depth [m]
h/L	Dispersion parameter [-]
$h_B$	Berm height [m]
$H_i$	Incident wave height [m]
$H_{m0}$	Wave height, zeroth moment of wave spectrum [m]
$H_{nom}$	Nominal wave height [m]
$H_r$	Reflected wave height [m]
$H_s$	Significant wave height [m]
IOW	Leibniz Institute for Baltic Sea Research, Warnemünde
$K_r$	Reflection coefficient [-]
$K_t$	Transmission coefficient [-]
L	Wave length [m]
q	Wave overtopping rate [ $l/(s \cdot m)$ ]
$q_{adm}$	Admissible wave overtopping rate [ $l/(s \cdot m)$ ]
$q_{max}$	Maximum waver overtopping rate [ $l/(s \cdot m)$ ]
SLR	Sea level rise
SWL	Still Water Level
$T_{01}$	Mean wave period, out of zeroth and first moment of wave spectrum[s]
$T_m$	Mean wave period [s]
$T_p$	Peak wave period [s]
u	Velocity [m/s]
$v_{max}$	Velocity [m/s]
$\gamma_b$	Berm factor [-]
$\theta$	Wave attack angle [ $^\circ$ ]
e.g.	for example (exempli gratia)
i.e.	that is (id est)

# 1 Introduction

## 1.1 Motivation and Objectives

The Falster Dike Board (FDB), advised by the Danish Coastal Authority (DCA), has commissioned the Leichtweiß-Institute to perform a safety assessment of the coastal protection system of the Falster coastal defence system, hereafter called “Falster Dike”. The main objective is to assess the reliability of the Falster Dike, which includes (i) the probability of failure of the most critical dike and dune sections and (ii) suggestions of possible countermeasures, based on the results under (i).

The desk study comprises three distinct phases: (i) collation and analysis of data, including generation of missing data, (ii) preliminary analysis of hydraulic boundary conditions and wave loading (runup and overtopping), and (iii) reliability analysis and counter measures. In a preliminary report (no. 001) first results of the safety assessment were shown. The final results of this study under current and future hydraulic conditions are presented in this report.

First, the topography and bathymetry of the Falster coastal protection system are described (section 2.1) and the hydraulic boundary conditions are assessed (section 2.2). As for the coastal protection system consisting of dike and dunes, three cases are considered for the dike in combination with dunes (chapter 3): (a) dunes without dike; (b) dike without dunes; (c) combination of dike and dunes (by means of a berm structure).

The sea state conditions have been simulated by the numerical model SWAN (section 4.1). The behaviour of dunes during storm surges was simulated by the numerical model XBeach (section 4.2). Afterwards, deterministic and probabilistic approaches were performed using the boundary conditions of the Falster Dike (section 4.3 and 4.4). The final results of the reliability assessment of the Falster Dike are summarised together with conclusions and recommendations in chapter 5.

## 1.2 Investigation Area

The southeast coastline of the island of Falster is shown in Fig. 1.1 together with the topography and bathymetry of the investigation area. The coastal protection system consists of a dike and natural dunes at seaside. For the safety assessment, the dike with a total length of 17.6 km was investigated. Similar sections of the dike were identified using the crest height and the

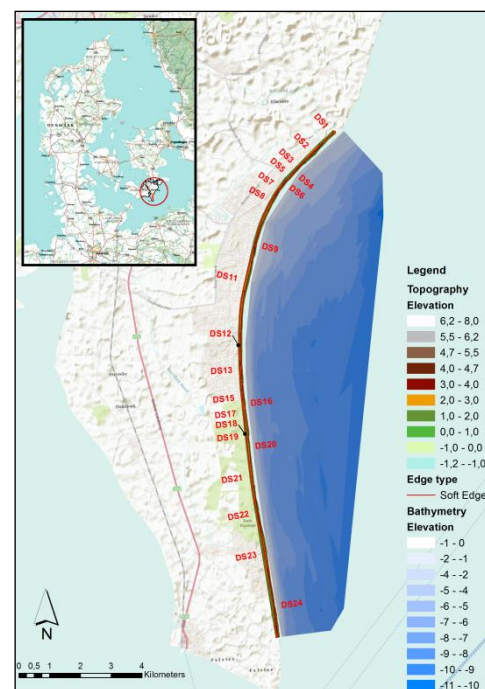


**Fig. 1.1: Investigation area with topography and bathymetry (Data source: DCA, 2011 and FDB, 2011)**

average dike slope (see section 2.1.1 and appendix A) so that the dike could be split into 24 sections which are all of different lengths but being considered homogeneous in itself (cf. Fig. 1.1).

## 2 Data Processing and Boundary Conditions

### 2.1 Topography and Bathymetry

#### 2.1.1 Topography of Dike and Dunes

Topography data from a LIDAR (light detection and ranging) survey was provided by the Falster Dike Board (FDB, 2011) and were processed with a geographic information system (cf. Fig. 2.1) to examine the following dike and dune characteristics:

- dike orientation (wave attack angle),
- dike height,
- seaward and shoreward dike slope,
- dune sand volume.

As mentioned before, the Falster Dike was divided alongshore into 24 dike sections from DS1 to DS24 (Appendix A). The dunes were categorized in three main dune sections from DI to DIII (Appendix A). The profile at the South end of the Falster dike and the dune crossing no. 5 in Marielyst were additionally analysed since they were believed to be the most critical cross profiles.

#### 2.1.2 Bathymetry

The bathymetry of Falster was determined by echo sounder profiles (DCA, 2011) and was extended by data from the Leibniz Institute for Baltic Sea Research Warnemünde, IOW (Seifert et al., 2001). These data were used to simulate the development of sea states, to simulate beach and dune erosion, and to calculate wave runup and mean wave overtopping rates. The bathymetry map of

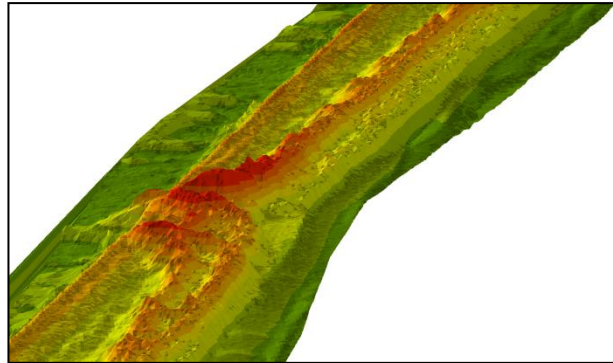


Fig. 2.1: Detail of topography of Falster Dike with dunes - example of crossing no. 5 in Marielyst (Data source: FDB, 2011)

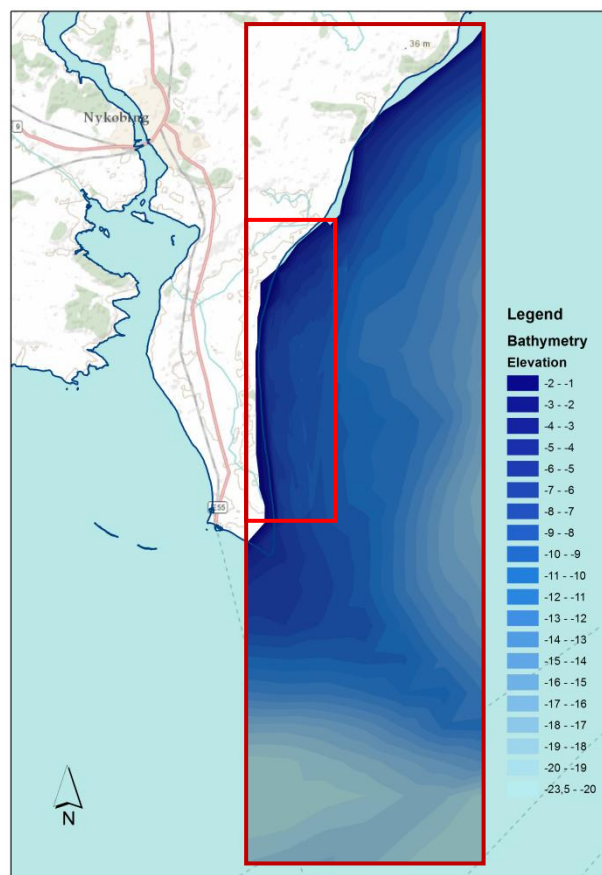


Fig. 2.2: Bathymetry of baltic sea at the Falster Island (Data source: DCA, 2011 and Seifert et al., 2001)

Falster is shown in Fig. 2.2 with an interpolated resolution of 500 m for the coarse grid and 100 m of the nested fine grid.

## 2.2 Hydraulic Boundary Conditions

### 2.2.1 Water Level and Storm Surge Scenarios

One of the most important parameters to determine the safety of the coastal protection system is the water level (Tab. 2.1). Four different water level scenarios were considered. Therefore, two different return periods and two different sea level rise (SLR) scenarios were taken into account. The sea level rise was considered to amount 30 cm for a period until 2055-2065 and 100 cm for a period until 2090-2100. The return periods were determined by statistical analysis of the water level of the gauges at Heasnes and Gedser (DCA, 2007).

Tab. 2.1: Water level scenarios

Scenario	Water level [m] <sup>1)</sup>	Return period [1/years]	Sea level rise (SLR)
A	1.50	1/20	hw <sub>20</sub> return period of 1/20
B	1.69	1/100	hw <sub>100</sub> return period of 1/100
C	1.99	1/100 + SLR <sup>2)</sup>	hw <sub>2065</sub> 1/100 water level + 30 cm (SLR)
D	2.69	1/100 + SLR <sup>2)</sup>	hw <sub>2100</sub> 1/100 water level + 100 cm (SLR)

<sup>1)</sup> based on the DVR90 reference level; <sup>2)</sup> SLR = sea level rise

The storm surge in 1872 reached a maximum water level of approximately 2.1 m at the Falster Dike (Rasmussen et al. (1997)) to 2.8 m at Køge Havn (DHI, 2006) at the eastern coastline of Falster. Therefore, since scenario D considered a very similar water level, it was believed that scenario D also includes calculations for the 1872 storm surge.

In order to consider not only the peak water level during a storm in the Baltic Sea, a time history of water level during a storm was considered. Therefore, a scenario was chosen with a total duration of 12 hours and with a duration of the maximum water level of 3 hours. For this purpose, a linear increase and a linear decrease of the water levels within 4.5 hours were assumed (cf. Fig. 2.3).

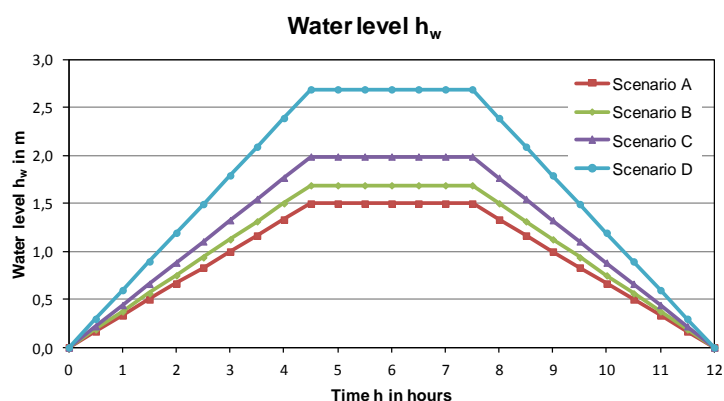


Fig. 2.3: Development of water level  $h_w$  of four storm surge scenarios

The time history of the water level was considered by the numerical dune erosion model to account for the temporal development of the beach and dune erosion. For the simulation of the sea state and for the calculation of wave runup and overtopping rates, a constant peak water level was assumed, hence assuming a conservative approach.

### 2.2.2 Wind Parameters

Wind data of the Denmark Meteorology Institute (DMI, 2011) for the stations ‚Gedser Havn‘ and ‚Gedser Odde‘ were analysed to determine the wind conditions at the island of Falster. Therefore, the wind speed was examined together with the wind direction (Kaste, 2011). The analysis of the wind data resulted in a maximum wind speed of 20.1 m/s in the range of wind direction of 0° (North) to 180° (South). For the calculation of sea states, the maximum wind velocity was set to the direction of 90° (East), again assuming the most conservative approach.

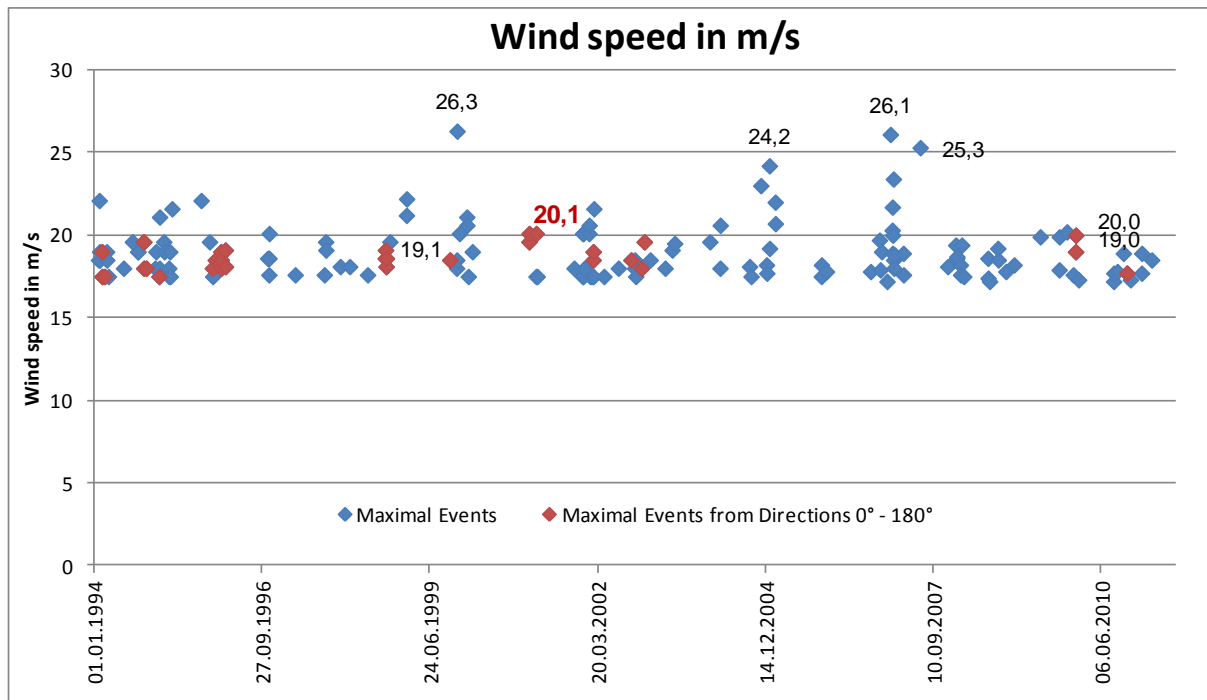


Fig. 2.4: Maximum wind speed from directions 0° - 180°

### 2.2.3 Sea State

The sea state was calculated starting from the coastline using a width of approximately 4 km offshore. The following main parameters were computed (using a resolution of 100 m):

- significant wave height  $H_{sig}$ ,
- peak wave period  $T_p$ ,
- wave attack angle  $\theta$ .

The results of the sea state computations are given in section 4.1 and Appendix B for each scenario A, B, C and D.

For the analysis of the sea state in front of the coast of Falster, the numerical model ‘SWAN’ (*Simulation WAves Nearshore* (SWAN, 2006)) was applied to simulate the specific local conditions. The results of this sea state model were used for the calculation of wave runup, wave overtopping rates, and for the simulation of dune erosion (cf. Section 4.1).

SWAN uses the spectral action balance equation to compute the evolution of wave growth. Terms of sources and sinks denote (SWAN, 2006):

- wave growth by the wind,
- nonlinear transfer of wave energy through three-wave and four-wave interactions,
- wave decay due to whitecapping,
- bottom friction,
- depth-induced wave breaking.

A JONSWAP-Spectrum was implemented as a boundary condition without any a priori restrictions of the spectrum. Therefore the significant wave height, the peak period and the wave direction are needed as an input. Further initial conditions are wind speed and wind direction (SWAN, 2006). For 2D-computations equidistant grids were defined. The optimal cell size was determined to be 50 to 100 m (Wahl, 2007). Therefore, a grid size of 100 m was chosen for the finer grid in front of the coastline. After the calculation of the sea state in a coarse grid, a finer grid next to the coastline is nested into the coarser model. The approach and the results of the numerical simulations with SWAN are shown in section 4.1.

The sea state parameters in a water depth of 10 m were calculated by SPM (1984) and EAK (2002) using a fetch length and wind speed, details of which are shown in Kaste, 2011). These results are used as the boundary conditions for the numerical model. In Tab. 2.2 an overview of the SWAN boundary conditions for the coarse grid is shown.

**Tab. 2.2: SWAN boundary conditions at offshore border**

<i>Parameter</i>	<i>Unit</i>	<i>Value</i>
Wave height $H_{sig}$	m	3.0
Wave period $T_p$	s	5.5
Wave angle $\theta$	°	90 (East)
Wind speed $U$	m/s	20.1
Wind direction	°	90 (East)

### 2.3 Beach and Dune Erosion

The calculation of dune and beach erosion was performed by the numerical model ‘XBeach’ (*eXtreme Beach behaviour*). The XBeach model simulates the behaviour of sandy coasts with given hydrodynamic parameters (wave height, wave period, water level, wind, currents, wave-current interaction etc.) and morphodynamic parameters (grain size, sediment transportation, erosion process, etc.). The numerical model performs well for dune erosion, overwash and breaching and was therefore selected suitable for the assessment of the Falster Dike reliability (Roelvink et al., 2010).

As one of the first models XBeach can calculate infragravity waves and wave group generated surf and swash motions which are found to be very important when it comes to dune erosion. Furthermore, XBeach provides an avalanching mechanism to simulate the slumping effects at the foredune during storm surge conditions (McCall et al., 2010). The computational simulation takes place in a 2DH environment. As input parameters an initial bathymetry and a grid system are defined. Hydrodynamic, morphodynamic and time parameters are set within the program. The main output is a time-varying bathymetry but also runup levels and temporal change of hydrodynamic and morphodynamic parameters are simulated.

The numerical model XBeach was developed by Unesco IHE, the Delft University of Technology, and Deltares, The Netherlands. XBeach was tested in several case studies as well as in experiments. It has been found that the physics of dune erosion, overwash, breaching, avalanching, swash motion, infragravity waves, wave groups, wave current interaction, as to name a few, during extreme storm conditions are reliably implemented in the model (Roelvink et al., 2010).

The dune at the South cape of Falster (South of Falster Dike) was calculated first as one of the probably critical cross sections. Therefore, the cross section of the dune and the bathymetry were prepared for the simulation of dune erosion. In addition, the dunes along the coastline were merged to three dune sections with the station marks as given in Tab. 2.3 (see also Appendix D). The dune crossing no. 5 in Marielyst was separately assessed because of a very low dune capacity. In Tab. 2.3 five dune profiles are shown with dune sections, station marks, and the corresponding dike sections (see also Appendix A).

**Tab. 2.3: Dune sections with stations marks**

<i>Dune profile</i>	<i>Dune section</i>	<i>Station mark</i>	<i>Dike section</i>
North	D I	0+000 to 3+500	DS02
Marielyst	D II	3+500 to 9+500	DS13
Marielyst Crossing No. 5	D II	4+800	DS09
South	D III	9+500 to 17+600	DS18
South End	D III	17+600	-

### 3 Methodology

The coastal protection system at the Falster Dike consists of a dike with natural dunes in front. On this account a separation of the coastal protection system was performed. The classification of the Falster Dike structure is shown in Fig. 3.1.

In a first step, the hydraulic boundary conditions were determined by water level statistics, wind parameters, topography and bathymetry. These parameters have been used to preliminarily determine the reliability of the Falster Dike by only taking into account the dike (and not the dune) and only considering wave overtopping simulations for four different water level scenarios (Kaste, 2011).

In the second step, the numerical model SWAN was applied to simulate the sea state in the nearshore area for the four water level scenarios as defined in Tab. 2.1. Deterministic and probabilistic approaches were then applied for the safety assessment of this protection system. Wave runup and wave overtopping rates with regard to the local boundary conditions were determined. The wave runup is measured vertically from the still water level. Wave overtopping describes the mean discharge of waves over the dike crest per meter width in  $l/(s\cdot m)$ . Two maximum admissible wave overtopping rates were selected as threshold values for the stability of the dike ( $0.5 l/(s\cdot m)$  and  $2.0 l/(s\cdot m)$ ).

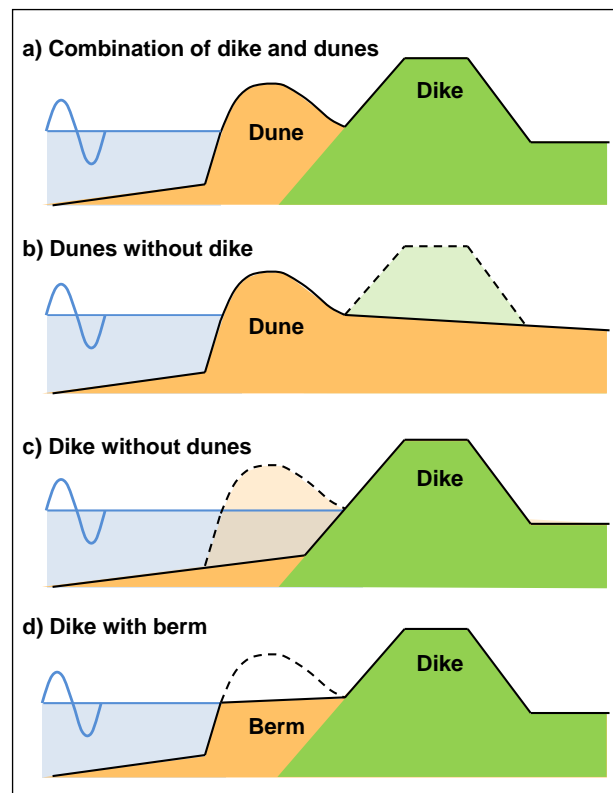


Fig. 3.1: Classification of coastal protection system

For the analysis of wave runup and wave overtopping rates, three different cases of the combined coastal protection system (Fig. 3.1 a) were determined:

- dunes without considering the dike (Fig. 3.1 b),
- dike without considering the dunes (Fig. 3.1 c),
- dike with a berm (combination of dike and dunes) (Fig. 3.1 d).

**Dunes without considering the dike:** The dunes were separately assessed for the simulation of wave runup, overwash and dune erosion. The beach and dune erosion was simulated by the numerical model XBeach. In order to minimize the simulation efforts, the dunes were divided into three dune sections using the key parameters ‘dune height’, ‘dune capacity’, and ‘distance between dunes and dike crest’.

**Dike without considering the dunes:** The dunes in front of the dike were neglected to determine the wave runup and wave overtopping rates for the dike. For each of the 24 dike sections the dike parameters were determined. Calculations of wave runup and wave overtopping rates were performed according to the EurOtop Manual (EurOtop, 2007).

**Combination of dikes and dunes:** an updated dike geometry with a berm was applied for calculating wave runup and wave overtopping rates (Fig. 3.1 d). The dike geometry was estimated from erosion simulations using XBeach and was simplified to a berm profile. This profile was assumed to no further erode and could therefore be used for wave run-up and overtopping simulations.

In a further step, the combined coastal protection system was assessed by a probabilistic approach. The failure probabilities were calculated by Monte-Carlo simulations with the software tool Palisade @Risk.

## 4 Results

### 4.1 Sea State Simulation with SWAN

For the calculation of the sea state at the coastline and offshore, the numerical model SWAN was applied. A fine and a coarse grid were interpolated from depth profiles. The characteristics of these grids are shown in Tab. 4.1.

**Tab. 4.1: Characteristics of the SWAN model grids**

<i>Description</i>	<i>Origin (UTM 32U)<sup>1)</sup></i>	<i>Cell count</i>	<i>Cell size</i>	<i>Width, Height</i>
	[m]	[-]	[m]	[m]
Coarse grid of the Baltic Sea determined by Seifert et al., 2001	$X_0 = 690985$	25 · 94	500	12000, 47000
	$Y_0 = 6033167$			
Fine grid interpolated of echo sounder profiles (DCA)	$X_0 = 691046$	46 · 163	100	4600, 16300
	$Y_0 = 6051928$			

<sup>1)</sup> refers to the upper left corner of the grid with UTM 32U coordinates

For the simulation of the wave conditions in the nearshore area, the fine grid was nested into a coarse grid to consider the offshore wave conditions. The wind (cf. section 2.2.2) and wave boundary conditions (cf. section 2.2.3) were applied to the eastern model border of the coarse grid (about 12 km offshore). In these grids, the wave parameters (e.g.  $H_s$ ,  $T_p$ ) were calculated for each cell, and the output was prepared for a longshore line with 100 m distance to the

coastline. These results were used for the calculation of wave runup and wave overtopping rates. The sea state parameters at the offshore boundary of the fine grid were then used for the simulation of dune erosion. In Fig. 4.1, the maximum wave height  $H_{sig,max}$  (determined as  $H_{m0}$  for XBeach) is shown for each dike section (for dike sections see Appendix A).

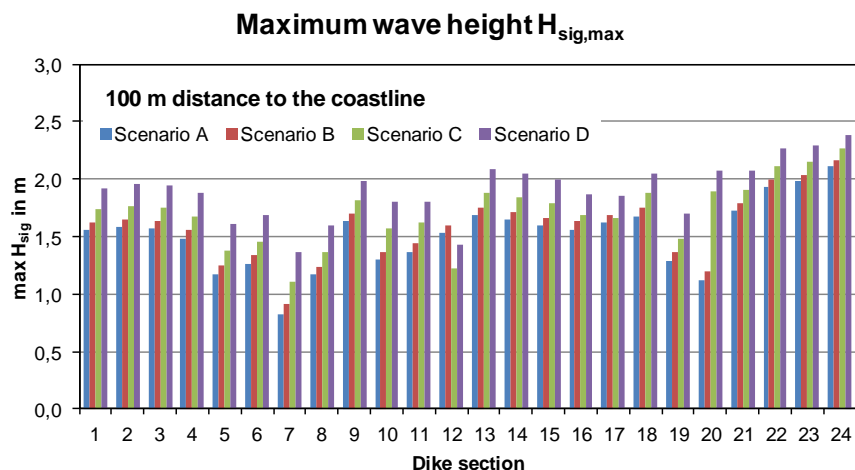


Fig. 4.1: Wave height  $H_{sig}$  for each dike section in a distance of 100 m to the coastline

It can be seen from Fig. 4.1 that the maximum significant wave height hardly exceeds 2.0 m at the shore which in most cases only occurs for Scenario D which is the highest water level (2.69 m DVR). The low values in dike section 7, 8 and 19, 20 result from a shallower bathymetry.

Fig. 4.2 shows the wave period  $T_{m01}$  in a distance of 100 m to the coastline for each dike section (for dike sections see Appendix A). In comparison with the boundary condition of the wave period at a distance of ca. 11 km offshore ( $T_{m-1,0} = 5.5$  s) a slightly lower wave period was calculated nearshore.

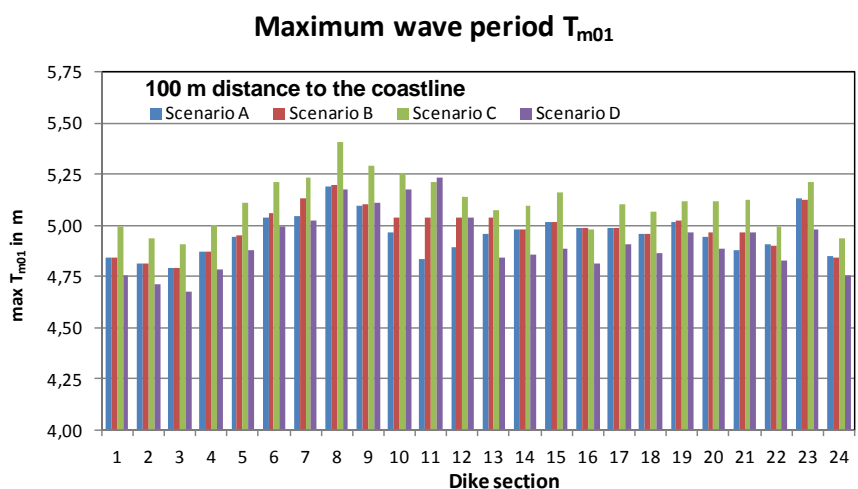


Fig. 4.2: Wave period  $T_{m01}$  for each dike section in a distance of 100 m to the coastline

It is surprising to see that Scenario C usually generates the highest wave periods. This is believed to result from the numerical calculation at the shore model boundary. In sections 8 and 9, wave periods are larger than in the other dike sections due to the swan friction model. In general, the SWAN model underestimates the simulated wave period (Wahl, 2007).

The wave attack angle, defined as the wave direction perpendicular to the coastline is given in Fig. 4.3. The dike sections are again given in ascending order from North to South.

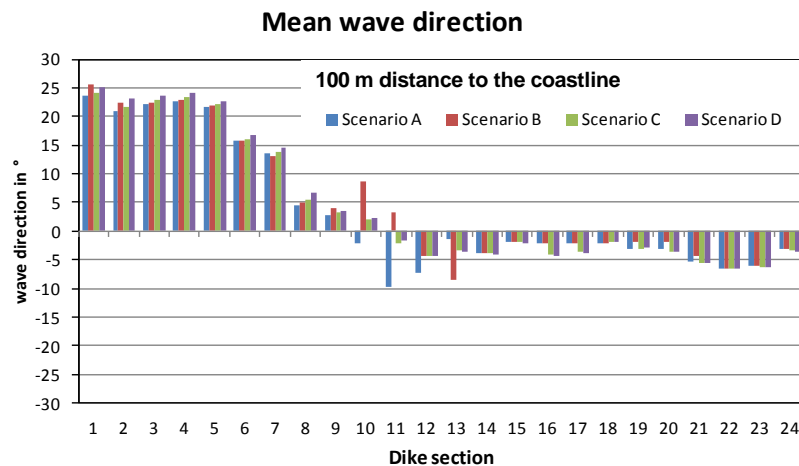


Fig. 4.3: Mean wave direction  $\theta$  for each dike section in a distance of 100 m to the coastline

In most cases (for dike sections 10 to 24), the wave attack is almost perpendicular to the coast whereas the northern part of the Falster Dike ranging from dike section 1 to 7 is mainly influenced by an oblique wave attack with a higher longshore component. It can be concluded, that in this case there exists a higher potential of sediment transport rates in longshore direction.

In the same way, the sea state parameters were extracted at the offshore boundaries of the echo sound profiles for numerical simulation of dune erosion with the model XBeach. For application of the dune erosion model XBeach, a relation of wave height  $H_{sig}$  to water depth  $d$  is used to calculate the temporal development of the wave height  $H_{sig}$  for each time step. In Fig. 4.4, the example of wave heights  $H_{sig}$  at the offshore boundary of dune section D II (station mark 9+000) are shown for each water level scenario (see also Appendix C).

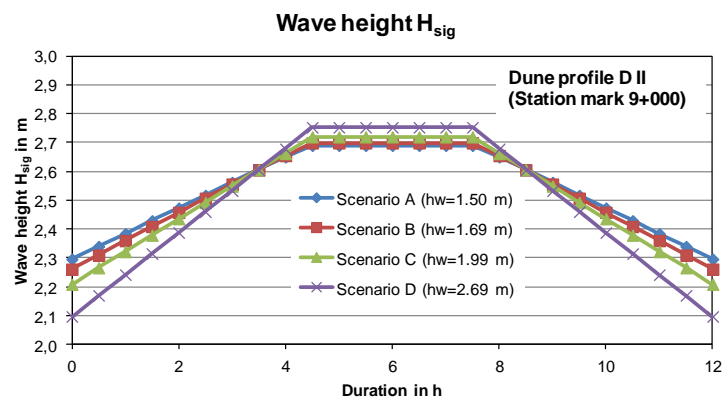


Fig. 4.4:  $H_{sig}$  at the model boundary of the cross profile 9+000

## 4.2 Simulation of Beach and Dune Erosion

### 4.2.1 Numerical Model XBeach

The dunes were analysed without consideration of the dike (cf. Fig. 3.1 c). For the calculation of dune and beach erosion, wave runup and overwash, the numerical model ‘XBeach’ (*eXtreme Beach behaviour*, cf. section 2.3) was applied. The dunes along the coastline were merged to three dune sections with following marks: DI 0+000 to 3+500, DII 3+500 to 9+000, DIII 9+000 to 17+600 (cf. Appendix A). For each dune section, the particular worst case cross section was chosen in respect to dune volume and dune height (Fig. 4.5, initial profile 1, 3, and 4, respectively). Therefore a GIS analysis of high resolution topography was performed to compare the characteristic of dune cross sections (see Fig. 2.1). Additional dune cross sections in DII and DIII were also chosen. Both additional profiles are quite unique because they either consist of an asphalt crossing (crossing no. 5 in Marielyst) through the dike-dune system in section DII (Fig. 4.5, initial profile 2) or they represent a dune at the South end of Falster where the dike line is missing, section DIII (Fig. 4.5, initial profile 5).

The wave parameters calculated by SWAN are used as hydraulic input parameters for the numerical XBeach simulations. Values between  $H_{m0} = 2.67 \text{ m} - 2.75 \text{ m}$  for the different cross sections located along the coastline were obtained. With respect to the different scenarios a rising water level of  $h_{w,100} = 1.69 \text{ m}$  in scenario B and  $h_{w,2100} = 2.69 \text{ m}$  in scenario D were estimated to analyse a high and an extreme storm surge event (cf. section 2.2). This was necessary to assess the safety of the combination of dike and dune. Scenario D was used to determine the maximum erosion profile for an assessment of the dike. The wave period  $T_p = 5.5$  and the simulated storm duration  $t = 12\text{h}$  remain constant for all simulation runs. A JONSWAP based wave spectrum and a morphological time factor “morfac factor” of 5 to speed up the morphological time were applied. This factor is a calibrated default parameter of XBeach to obtain realistic dune erosion profiles.

A sieve sample analysis of dune sand material next to crossing no. 5 in Marielyst yields a mean grain diameter  $d_{50} = 0.2 \text{ mm}$  with  $d_{90} = 0.3 \text{ mm}$ . The uniformity of the dune sand was determined to  $C_u = 1.8$ . These characteristics were taken into account as an input for XBeach.

### 4.2.2 Dune Erosion

Five different representative dune cross profiles were determined (section 4.2). For each cross profile, storm surge scenario B and D (section 2.2) were simulated by XBeach. The initial profile (green) and the erosion profiles for scenario B (blue) and D (red) are shown in Fig. 4.5, respectively where the y-axis represents the dune height and the x-axis represents the distance to the coastline as defined in Appendix A. Additionally, the erosion profiles are given in Appendix D in a larger version.

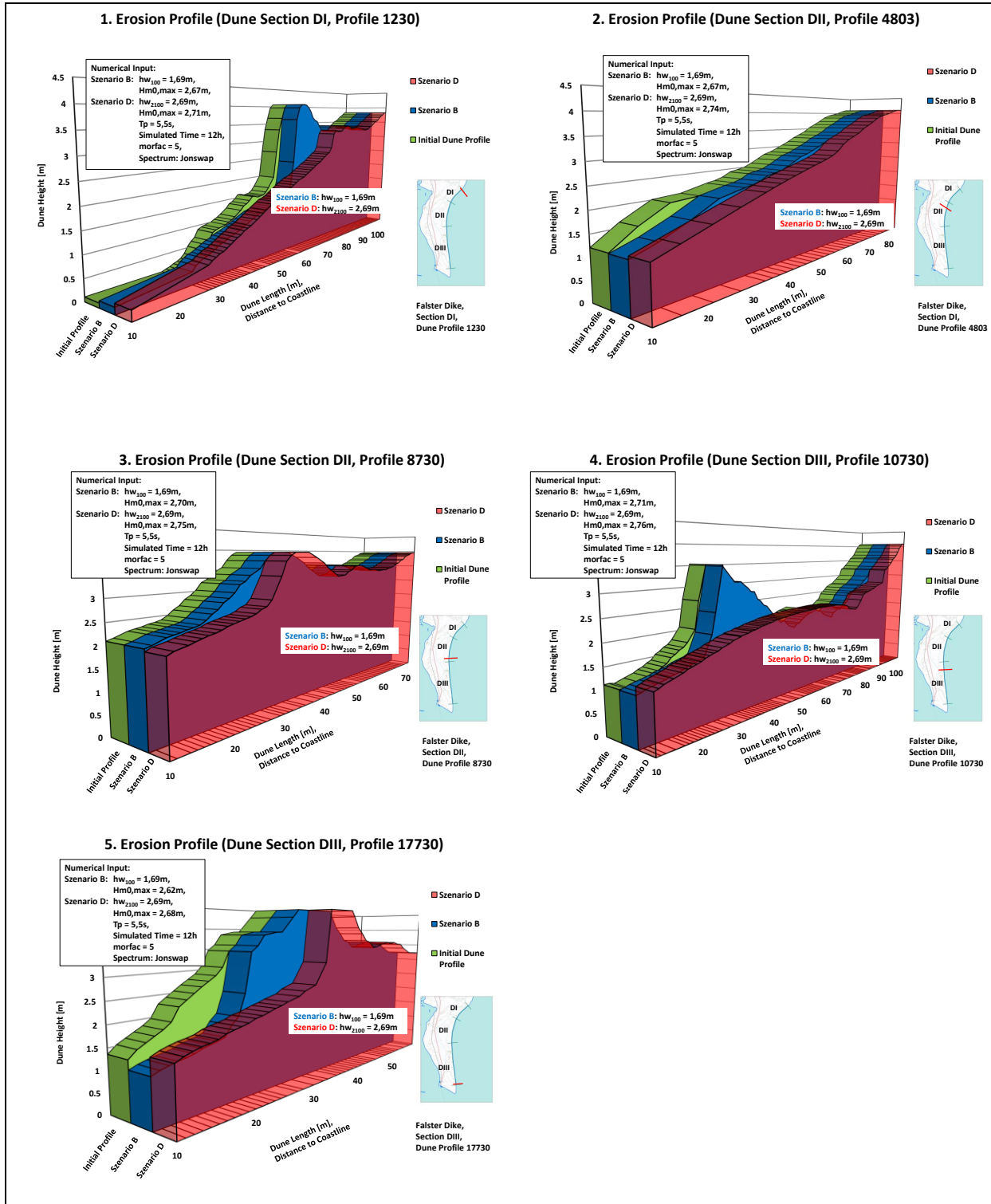


Fig. 4.5: Initial and erosion profiles of each dune profile

It can be seen from Fig. 4.5, that only small erosion volumes at the dune toe were observed for each cross section profile for storm surge scenario B. This means that the dunes are not eroded under these conditions and therefore do not lose their function.

In Scenario D, the erosion volume increases significantly as compared to scenario B for each cross section profile (Fig. 4.5). In case of the 4th erosion profile (Fig. 4.5, erosion profile 4)

the dune is completely eroded and a berm like structure has been generated. Once the dune is fully eroded only the dike line behind in combination with the created berm structure protects the hinterland from flooding. This is considered the worst case scenario and used for further calculations.

Regarding the two additional cross sections, the crossing in Marielyst (Fig. 4.5, erosion profile 2) and the cross section at the south end without the dike behind (Fig. 4.5, erosion profile 5), no significant changes with respect to the erosion volumes are observed. In the first case, hardly any erosion is visible which is due to the shallow dune front in this area. Therefore, wave runup is most likely the critical factor. In the latter case, approximately half of the dune cross section is eroded, leaving the other half of the dune to protect the hinterland from flooding.

### 4.2.3 Wave Runup and Overwash

Wave runup is calculated by an internal function of the XBeach program (Roelvink et al., 2010). For each time step, the last wet point on the beach is provided and interpreted as the actual wave runup. The maximum runup and the corresponding time can be found by analyzing the whole time series.

For each cross section this wave runup is calculated for scenario B (blue) and scenario D (red). All figures are given in Appendix E. For further analysis, only the worst case scenario (Fig. 4.5, erosion profile 4) from the erosion analysis and the two additional profiles in Marielyst (Fig. 4.5, erosion profile 2) and the dune without dike (Fig. 4.5, erosion profile 5) were investigated.

Wave runup, overwash and dune breach for the worst case scenario D (Fig. 4.5, erosion profile 4) are shown in Fig. 4.6 for dune section DIII.

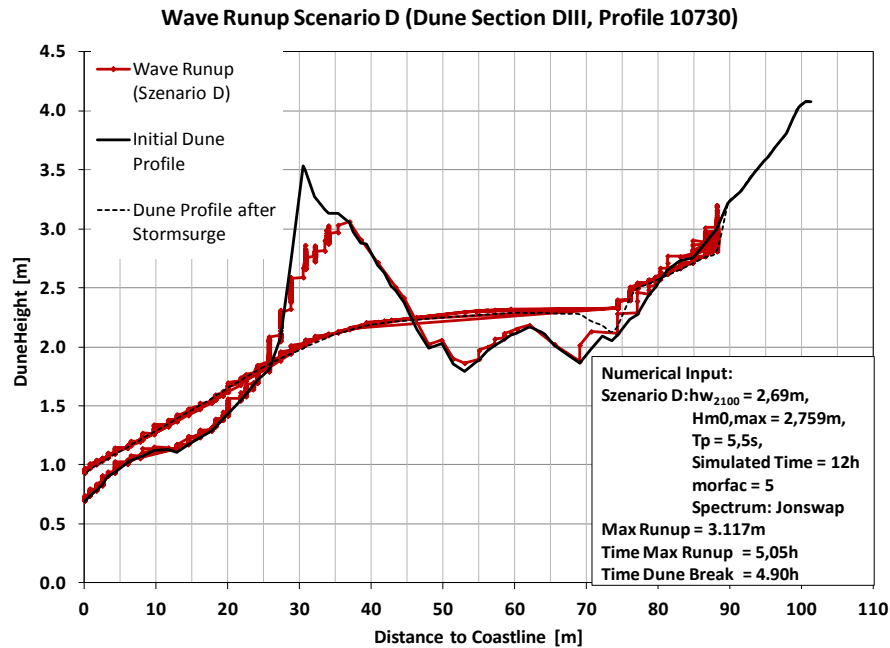


**Fig. 4.6: Wave runup and dune breach, 4<sup>th</sup> erosion profile dune section DIII and scenario D**

In Fig. 4.6, wave runup can be observed in front of the dune, followed by erosion and overwash of the dune. After a storm surge duration of 4.9 hours the dune breaches and wave runup occurs for the next 7.1 hours on the dike, resulting in erosion of the dike. The maximum wave runup is about 3.1 m which is still approximately 1.0 m lower than the dike crest. After the storm, when the water level is lowered again to mean water level, the dune is fully eroded and displaced and the sand forms a berm structure in front of the dike.

Wave runup for the two additional profiles in Marielyst (Fig. 4.5, erosion profile 2) and the dune without dike (Fig. 4.5, erosion profile 5) for scenario D are given in Fig. 4.7. In the case of Marielyst a maximum wave runup of 3.2 m is observed, approximately 1.0 m lower than the dike crest. This is of major importance for the crossing, since there is no dune protection in front and a relatively low slope. In the case of the dune at the Falster south end with no dune behind a maximum wave runup of 3.2 m is observed, which is approximately 1.8 m lower than the top of the dune. In both cases only wave runup and no overwash is observed, so that there will be no flooding of the hinterland.

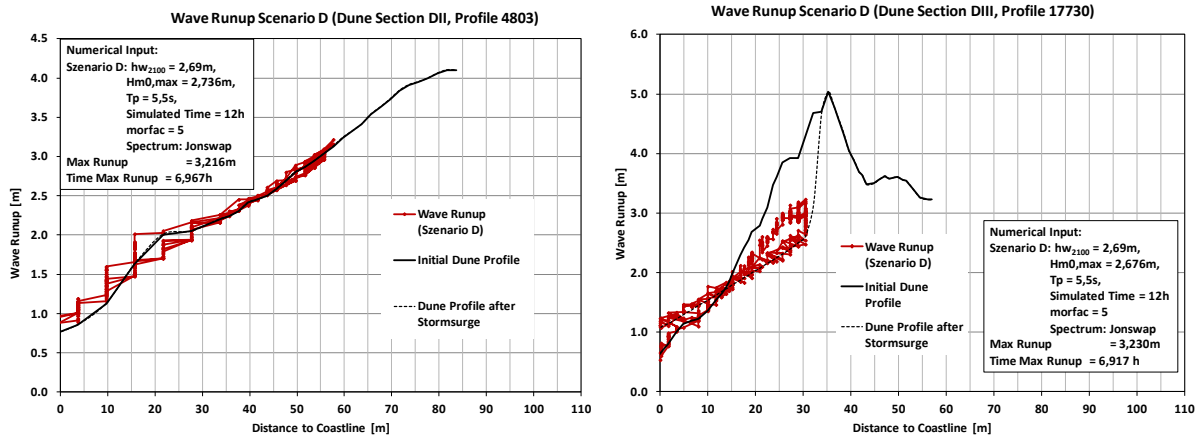


Fig. 4.7: Wave runup at crossing Marielyst (left) and Falster south end (without dike behind) (right)

#### 4.2.4 Dune Crossing

As an example of a dune crossing, the biggest crossing, no. 5 in Marielyst, was chosen. The XBeach model was used to determine the wave runup and erosion for this special geometry. Considering an asphalt cover layer at the crossing no. 5 in Marielyst, the erosion profile in Fig. 4.8 is determined. The simulation was run two times for the same profile. First, with a non erodible asphalt layer and second, with erodible sand material as bottom layer. The results are shown in Fig. 4.8. In the first case no erosion occurred in the area which was covered by asphalt but at the seaward end of the asphalt layer and in the latter case some erosion over a longer distance was observed.

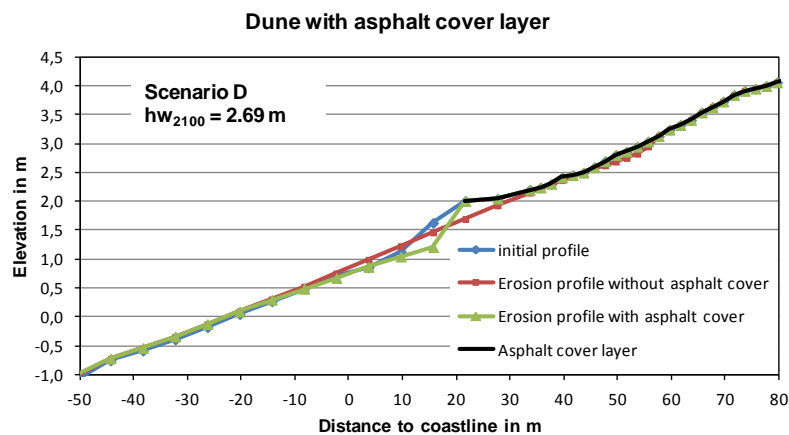


Fig. 4.8: Dune with asphalt cover layer at crossing no. 5 in Marielyst

#### 4.2.5 Summary of Beach and Dune Erosion

The assessment of dunes was performed by the numerical model XBeach with the storm surge scenarios B and D. No overwash and no wave overtopping was determined for the dunes in storm surge scenario B and the dunes in all dune sections resisted the load of scenario B (see Fig. 4.5).

Considering the dune crossing in Marielyst and storm surge scenario D it was observed that increased erosion occurs at the seaward end of the asphalt layer. Only wave runup but no overwash (no wave overtopping respectively) was observed.

Considering the dune cross section at the South end of the Falster Dike, without a dike structure behind and storm surge scenario D, it was observed that approximately 50% of the dune was eroded. Only wave runup and erosion but no overwash was observed.

For the worst case cross section profile and scenario D (Fig. 4.5, erosion profile 4) the dune was fully eroded and parts of the dike were eroded as well. After the storm surge, a berm like structure in front of the dike was observed. For further analysis the combination of berm and dike as a worst case scenario will be investigated (section 4.3.2 and section 4.4.1).

### 4.3 Deterministic Analysis of Wave Loading

The following three cases discussed in chapter 3

- dunes without considering the dike (Fig. 3.1 b),
- dike without considering the dunes (Fig. 3.1 c),
- dike with a berm (combination of dike and dunes) (Fig. 3.1 d).

will be analysed with respect to wave runup and mean wave overtopping rates in this section. All four scenarios for water levels are considered for each of these three cases and will be discussed in the subsections below.

#### 4.3.1 Assessment of Dike without Considering Dunes

In this section, the dunes in front of the dike were neglected for the calculation of wave runup and wave overtopping rates. For each section, the dike slope on the seaward side is determined using the cross profile from the topography in this section. Calculations were performed according to the EurOtop Manual (EurOtop, 2007). The wave overtopping rates for scenario A, B, C and D are shown in Fig. 4.9 together with the two admissible wave overtopping rates of 0.5 l/(s·m) and 2.0 l/(s·m).

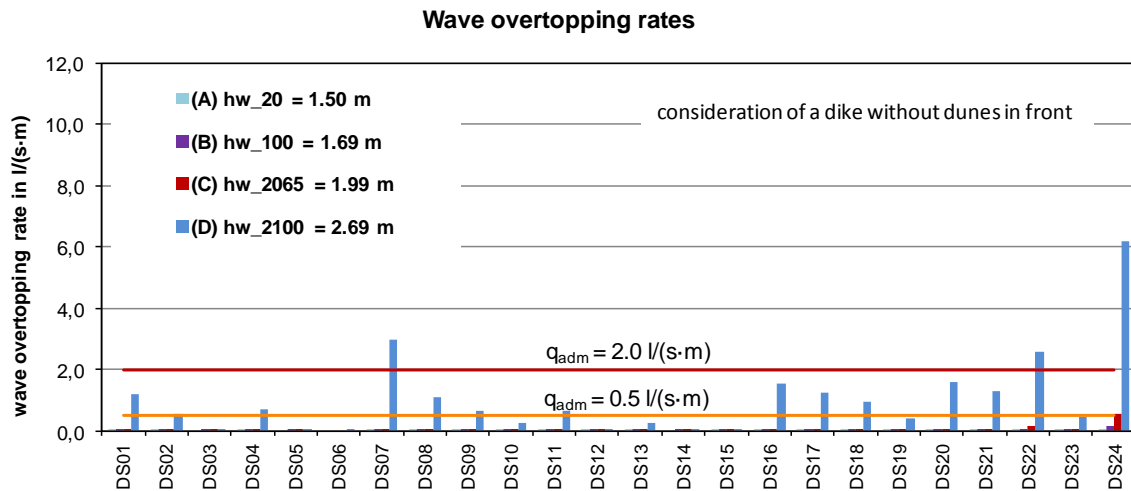


**Fig. 4.9:** Calculated maximum wave overtopping rates ordered by dike sections for each water level scenario with updated dike slopes [ $q_{\max} = 6.1 \text{ l/(s·m)}$ ]

Dike section DS07, DS22 and DS24 exceeded the admissible wave overtopping rate of  $2.0 \text{ l/(s·m)}$  for the worst case scenario D. Mainly influenced by the outer dike slope, these dike sections are the most critical sections. For all other scenarios the maximum wave overtopping rate amounted to  $0.6 \text{ l/(s·m)}$  and were therefore always below  $2.0 \text{ l/(s·m)}$ .

### 4.3.2 Assessment of Dike with Berm

To consider a combination of dike and dune, the dune erosion model was applied to three dune sections (DI, DII, DIII) as described in section 2.3. Therefore, the wave overtopping parameters were revised with respect to the berm in front of the dike. In Appendix B, examples of the determination of the berm are shown. A berm in front of the dike reduces the wave runup and mean wave overtopping rates. Fig. 4.10 shows an example of determining the berm and dike parameters at dune section DI.

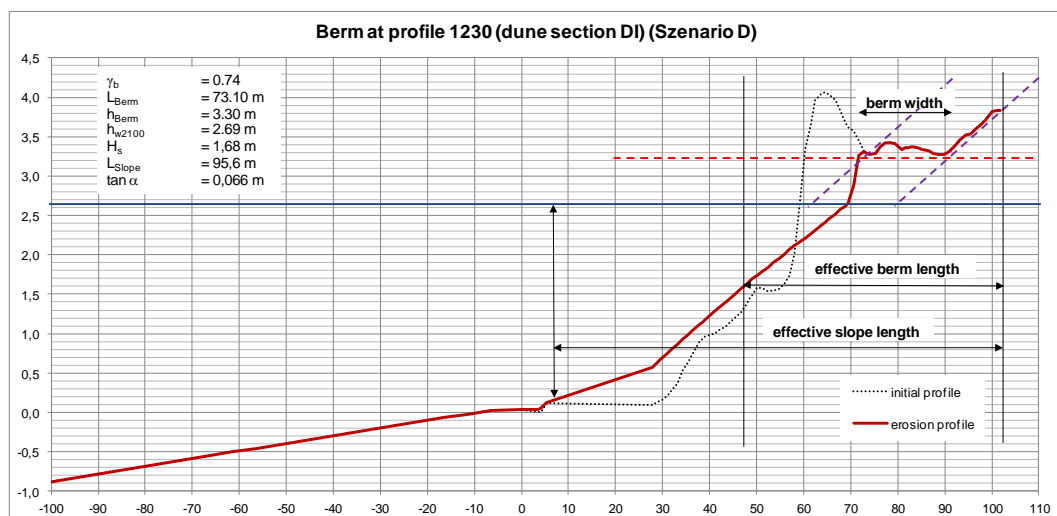


**Fig. 4.10:** Determination of effective berm length and berm width (dune section DI) (Scenario D)

In Figures 4.11 to 4.14 the berm factor  $\gamma_b$  is shown for scenario A, B, C and D for each dune section. Due to the changing water level for each of these scenarios, the berm factor is changing for each of them. Furthermore, it should be noted that the water level was kept constant for all calculations performed here. This is a conservative approach since the water level will change over time (as indicated in Fig. 2.3) so that the calculated results for wave runup and overtopping will only be valid during the maximum peak water level and are considered to be significantly lower during all other times.

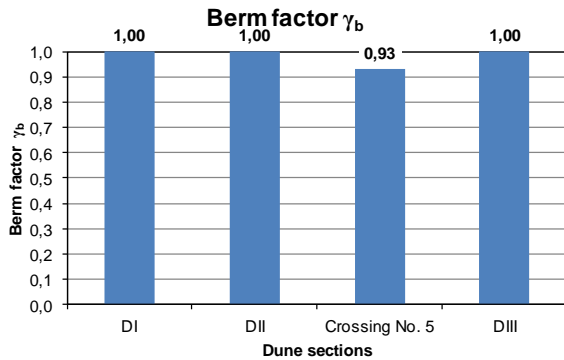


Fig. 4.11: Berm factor  $\gamma_b$  for each dune section (Scenario A)

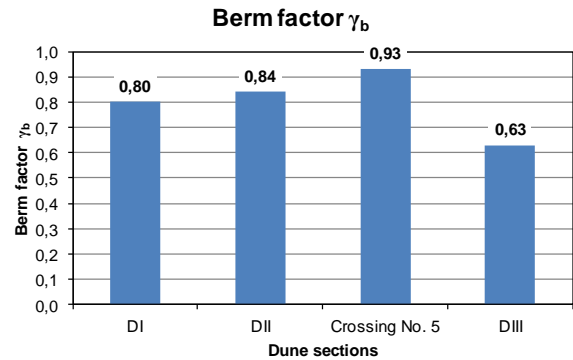


Fig. 4.12: Berm factor  $\gamma_b$  for each dune section (Scenario B)

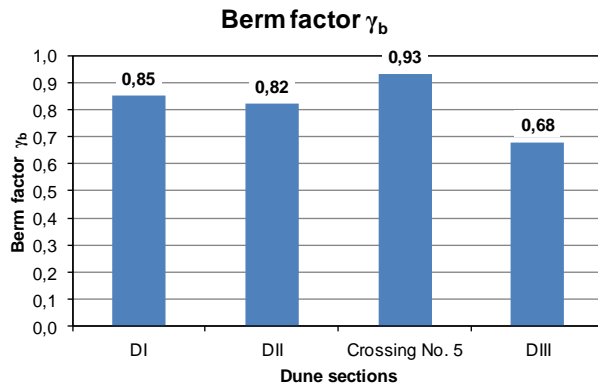


Fig. 4.13: Berm factor  $\gamma_b$  for each dune section (Scenario C)

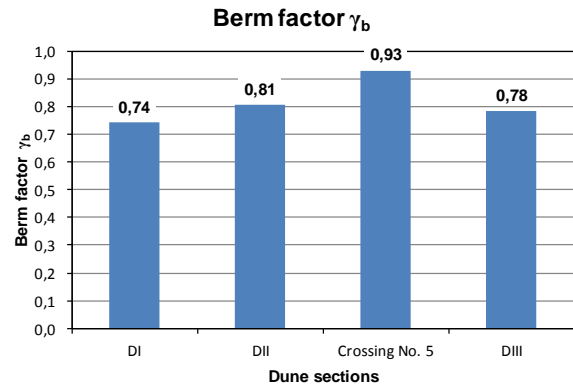
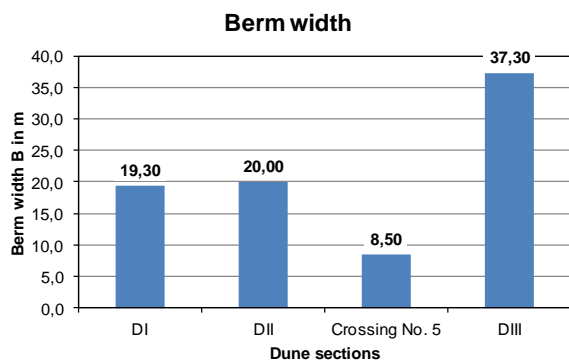
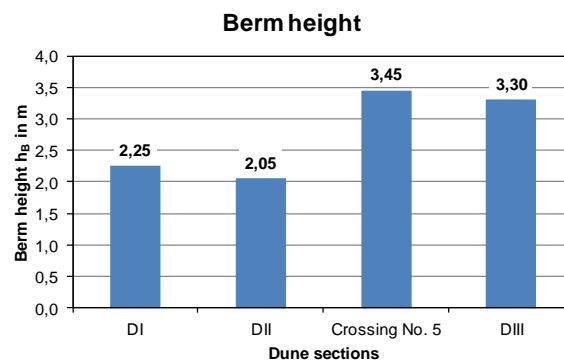
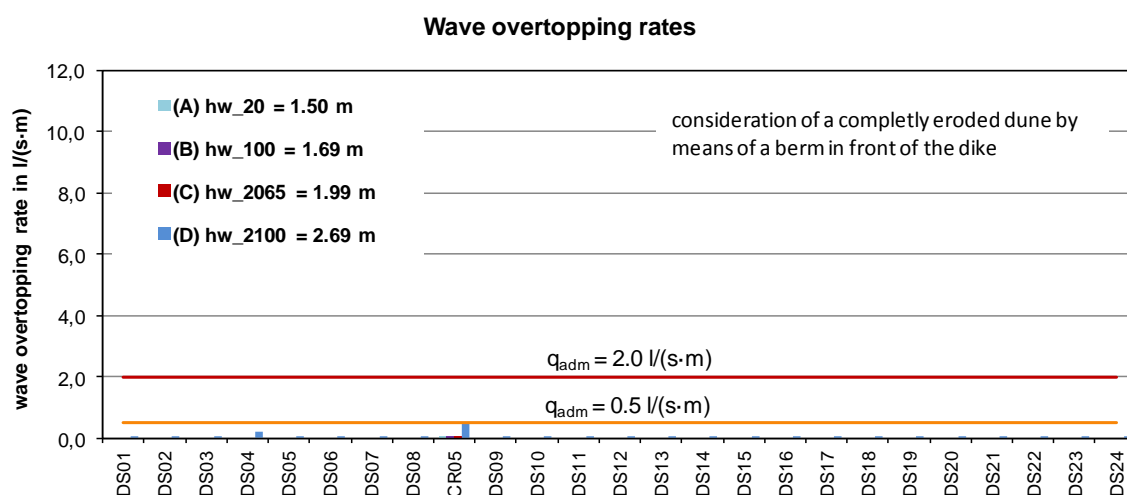


Fig. 4.14: Berm factor  $\gamma_b$  for each dune section (Scenario D)

In Fig. 4.15 the berm width is shown. From North to South the berm width is increasing by a larger distance between dune and dike. In addition, the berm height of each dune section is shown in Fig. 4.16.


 Fig. 4.15: Berm width  $B$  for each dune section

 Fig. 4.16: Berm height  $h_B$  for each dune section

Considering these berm factors the wave overtopping rates were calculated for each scenario. In Fig. 4.17 the maximum wave overtopping rates (after completely eroded dunes) are shown. The mean dike slopes with a effective berm length were taken into consideration.


 Fig. 4.17: Calculated maximum wave overtopping rates ordered by dike sections for each water level scenario with consideration of completely eroded dunes [ $q_{max} = 0.5 \text{ l/(s-m)}$ ]

For the case of a completely eroded dune, a berm will stay in front of the dike. This case yields a much lower wave runoff and mean wave overtopping rate. A larger distance between dune and dike also decreases the wave runoff and wave overtopping rate because of a larger berm width and a shallower dike slope. With respect to the berm height, a value of the highest water level is the most effective berm height for decreasing the wave runoff and wave overtopping rates. Dune section DIII has a lower lying theoretical berm height which leads to a higher potential wave runoff and wave overtopping rate compared to dune section DI and DII (see Appendix B).

Through the combination of dike and dune, it is concluded, that there is a considerable extra safety of the dike by the dunes in front. Even if the dunes are entirely eroded, the berm in

front of the dike reduces the wave overtopping rate. At the crossing no. 5 in Marielyst, the highest wave overtopping rate is calculated, with  $q_{\max} = 0.5 \text{ l/(s}\cdot\text{m)}$ . No wave overtopping rate exceeds the admissible values.

## 4.4 Probabilistic Analysis of Wave Loading

### 4.4.1 Assessment of Dike with Berm

A probabilistic approach was applied with using the software tool Palisade @Risk by means of a Monte-Carlo-Simulation. In a first approach the dunes were neglected for the probabilistic calculation (cf. Fig. 3.1 c). A maximum failure probability  $P_f = 0.43$  results for dike section DS18 when only wave overtopping is considered as failure mode and when applying a scenario with a water level of  $h_{w100} = 2.28 \text{ m}$  (Kaste, 2011). Furthermore, relatively high failure probabilities due to wave overtopping were determined for DS19, DS20, DS22 and DS24.

In the next step, in regard to section 4.3.2, the probabilistic approach was applied to the combination of dike and dunes (cf. Fig. 3.1 d) taking into account the failure mechanisms ‘wave overtopping’, ‘overflow’ and ‘erosion of outer dike slope’. The fault tree with the main failure mechanisms is shown in Appendix F.

The berm factors  $\gamma_b$  for each dune section related to the dike sections were taken into account for the scenario D. Fig. 4.18 shows the berm factors for scenario D for each dune section. The smaller the berm factor  $\gamma_b$  the smaller the wave runup and the wave overtopping rate respectively.

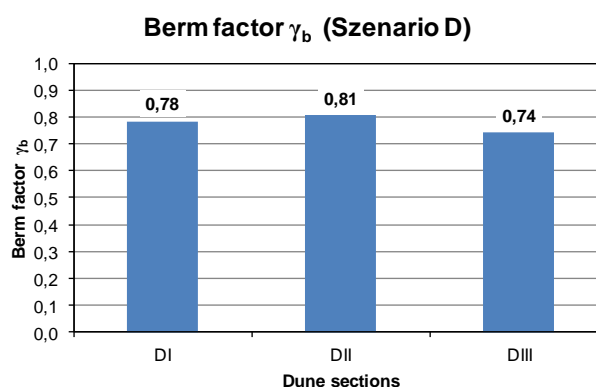


Fig. 4.18: Berm factor for each dune section (percentage rate of berm influence) (Scenario D)

### 4.4.2 Probability Calculation

The case of a dike with completely eroded dunes is applied for the probabilistic analysis (cf. section 4.3.2). Therefore, there are changes in the geometry of the dike as compared to previous probability calculations and which have been already discussed in section 4.3.1. Tab. 4.2 lists results of probability calculations for all dike sections employing the berm factors from the fully eroded dunes. These probability calculations include additional failure modes (cf. Appendix F) than discussed before but also the previously considered ones (‘wave overtopping’, ‘overflow’ and ‘erosion of the outer dike slope’). A critical overtopping rate was defined as  $0.5 \text{ l/(s}\cdot\text{m)}$ .

**Tab. 4.2: Results of probability calculation**

Probability	DS 1 – DS 24 Pf
Inundation	0.00E+00
Overflow	0.00E+00
Wave overtopping	0.00E+00
Dike breach	0.00E+00
Erosion seaward slope.	0.00E+00
Erosion landward slope	0.00E+00
Failure inner dike	0.00E+00
Failure dike top	0.00E+00

It can be seen that there is no failure probabilities calculated for the aforementioned conditions which means that the failure probabilities are smaller than  $P_f = 10^{-10}$ .

## 5 Conclusions, Recommendations and Outlook

The reliability of Falster Dike as a coastal defence system was assessed, which includes the probability of failure of the most critical dike and dune sections. The objective is to determine suggestions of possible counter-measures based on the results of the safety assessment. The desk study comprised three distinct phases: (i) collation and analysis of data, including generation of missing data, (ii) preliminary analysis of hydraulic boundary conditions and wave loading (runup and overtopping), and (iii) reliability analysis and counter-measures.

In chapter 2 the data processing of topography, bathymetry and hydraulic conditions was described together with the used software tools. The safety assessment was performed with deterministic and probabilistic approaches by four storm surge scenarios and three different cases: (i) dunes without considering the dike, (ii) dike without considering the dunes, (iii) combination of dike and dunes by means of a seaside berm structure (cf. chapter 3).

At first it is concluded, there is no proper exceeding of the admissible wave overtopping rate ( $q_{adm1} = 0.5 \text{ l/(s}\cdot\text{m)}$ ). No urgent hazard exists in regard to the wave overtopping rates at that time. Under current conditions the safety of the coastal protection system is sufficient. In the context of future conditions with a sea level rise in 2090 to 2100, wave overtopping rates exceeding the admissible value are predicted.

The present state of the analysis of the Falster Dike suggests the following conclusions:

- if only the dike is considered there is no significant wave overtopping for scenario A, B, C while scenario D may lead to wave overtopping rates up to  $6.2 \text{ l/(s}\cdot\text{m)}$ ,
- the combination of dune and dike adds a significant extra safety so that there is no immediate need for any countermeasures to be installed.

Potential weak spots for the worst case scenario D:

- Dune crossings, especially crossing no. 5 in Marielyst
- Dune section DIII at the south end of the Falster Dike
- Dike section DS7, DS9, DS22 and DS24

### **Recommendations**

The assessment of the coastal protection system of South Falster results in following recommendations: (i) no immediate action in dike reinforcement is required, (ii) constant maintenance of dike and dunes and (iii) consideration of improving the dune at the south end is recommended.

## Literature

- DCA (2007): Hojvandsstatistikker - Extreme sea level statistics for Denmark. Danish Coastal Authority, Lemvig, Denmark.
- DCA (2011): Data of echo sounder measurements at east coast of Falster Island, Danish Coastal Authority, Lemvig, Denmark. unpublished.
- DHI (2006): Vandstandsstatistik for Koege Havn. DHI Institut for Vand og Miljø, Horsholm, 16 p.
- DMI (2011): Wind data of Gedser Havn (01.01.06-31.08.11) and Gedser Odden (01.01.94-31.08.11), Danmarks Meteorologiske Institut (DMI).
- EAK (2002): Empfehlungen für Küstenschutzwerke. Heide i. Holst., Germany: *Die Küste. Archiv für Forschung und Technik an der Nord- und Ostsee*, Heft 65, Boyens & Co., 589 S.
- EurOtop (2007): European Overtopping Manual. Pullen, T.; Allsop, N.W.H.; Bruce, T.; Kortenhaus, A.; Schüttrumpf, H.; Van der Meer, J.W.; Kuratorium für Forschung im Küsteningenieurwesen: *Die Küste*, Heft 73, [www.overtopping-manual.com](http://www.overtopping-manual.com).
- FDB (2011): Topography data of coastline of Southeast Falster, Falster Dike Board (FDB).
- Kaste, D. (2011): Safety Assessment of the Coastal Protection System at Falster, Denmark. *Diplomarbeit am Leichtweiß-Institut für Wasserbau, Fachbereich Bauingenieurwesen, Technische Universität Braunschweig*, Braunschweig, Germany, 49 p., 10 appendices, D-7/2011.
- McCall, R.T.; van Thiel de Vries, J.S.M.; Plant, N.G.; van Dongeren, A.R.; Roelvink, J.A.; Thompson, D.M.; Reniers, A.J.H.M. (2010): Two-dimensional time dependent hurricane overwash and erosion modeling at Santa Rosa Island. *Coastal Engineering*, 57 (2010), 668-683.
- Rasmussen, F.F.; Dreijer, K.; Jørgensen, G. (1997): Det falsterkse dige. Nykøbing Falster, 96 p.
- Roelvink, D.; Reniers, A.; van Dongeren, A.; van Thiel de Vries, J.; Lescinski, J.; McCall, R. (2010): XBeach Model Description and Manual. Unesco-IHE Institute for Water Education, Deltares and Delft University of Technology, 1002266, Delft, 106 p.
- Seifert, T.; Tauber, F.; Kayser, B. (2001): A high resolution spherical grid topography of the Baltic Sea - 2nd edition. *Baltic Sea Science Congress, 25-29. November 2001*, Stockholm Poster #147.
- SWAN (2006): SWAN Scientific and technical documentation. Delft University of Technology, Delft, Netherlands, 126.
- Wahl, T. (2007): Ermittlung von Seegangsbelastungen im Küstennahbereich mit dem numerischen Seegangsmodell SWAN. *Diplomarbeit am Forschungsinstitut Wasser und Umwelt, Abt. Wasserbau & Hydromechanik der Universität Siegen*, Siegen, 161 S.

### Internet:

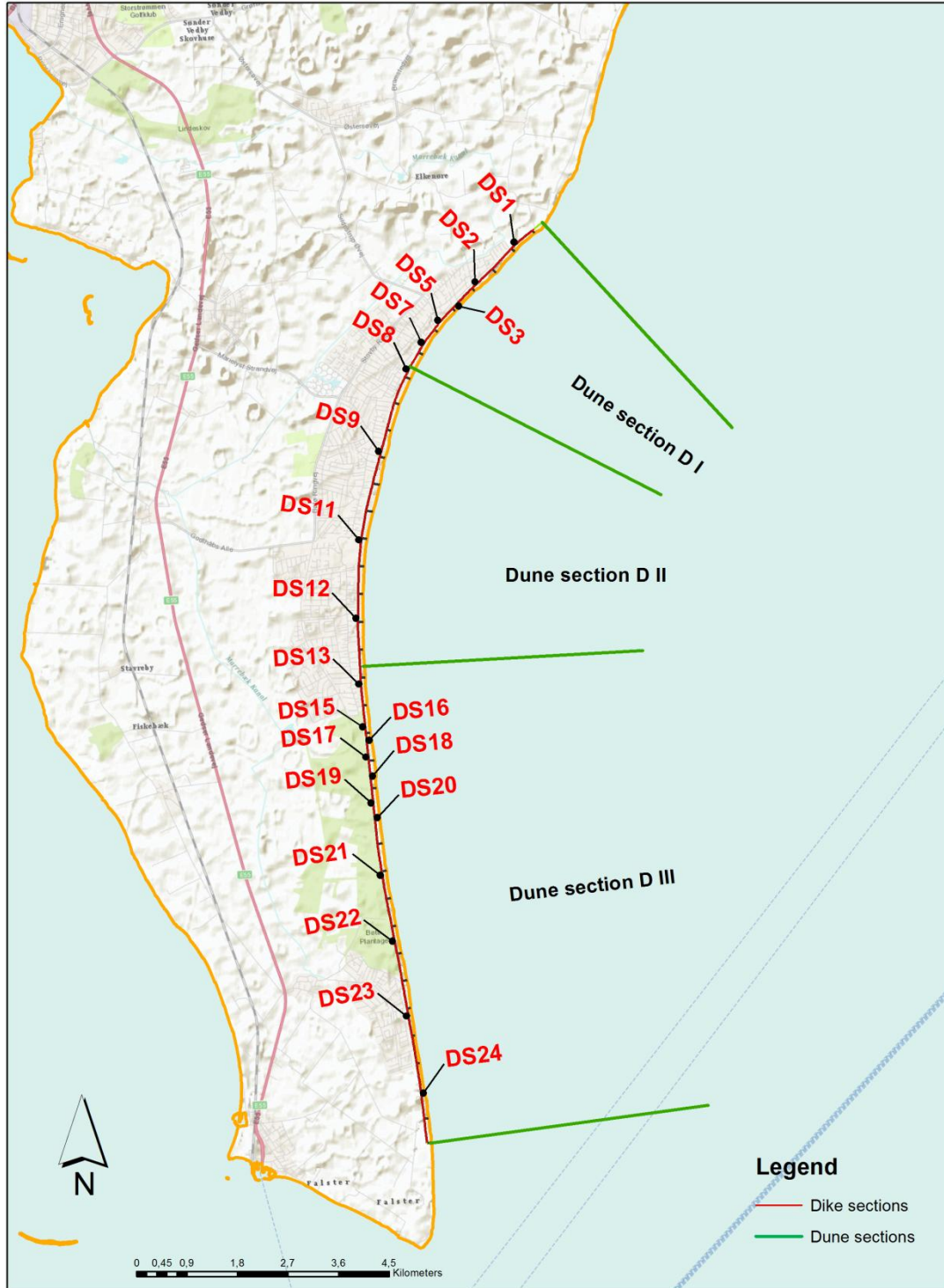
World Topographic Map:

[http://services.arcgisonline.com/ArcGIS/rest/services/World\\_Topo\\_Map/MapServer](http://services.arcgisonline.com/ArcGIS/rest/services/World_Topo_Map/MapServer)

## **Appendix**

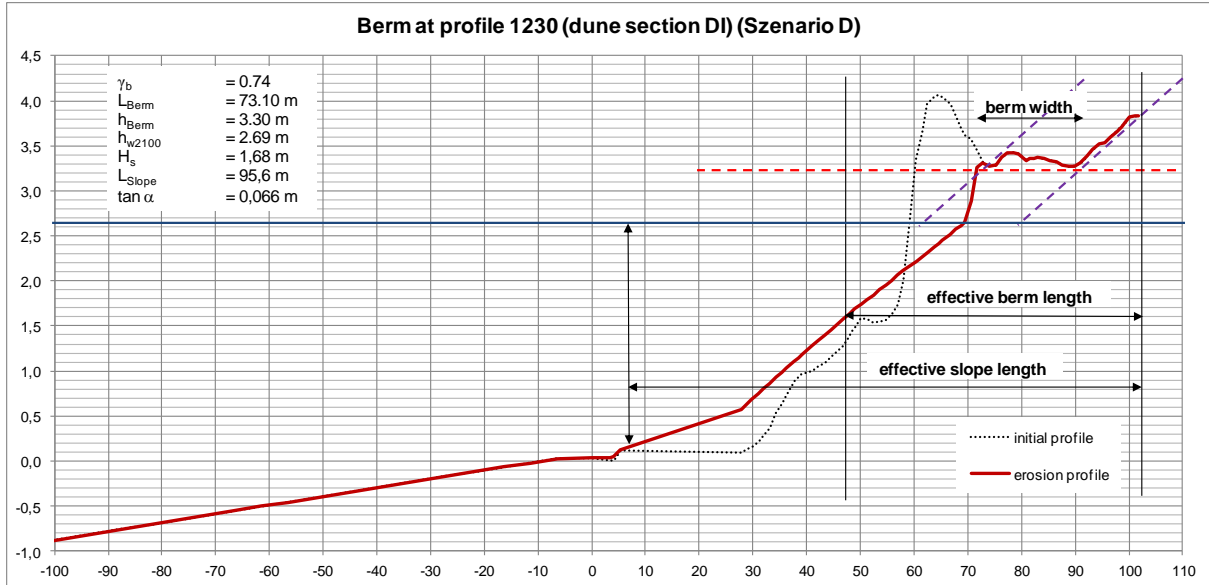
## Appendix A: Overview of Dike and Dune Sections

### Overview of dune sections (DI - DIII) and dike sections (DS1 - DS24)

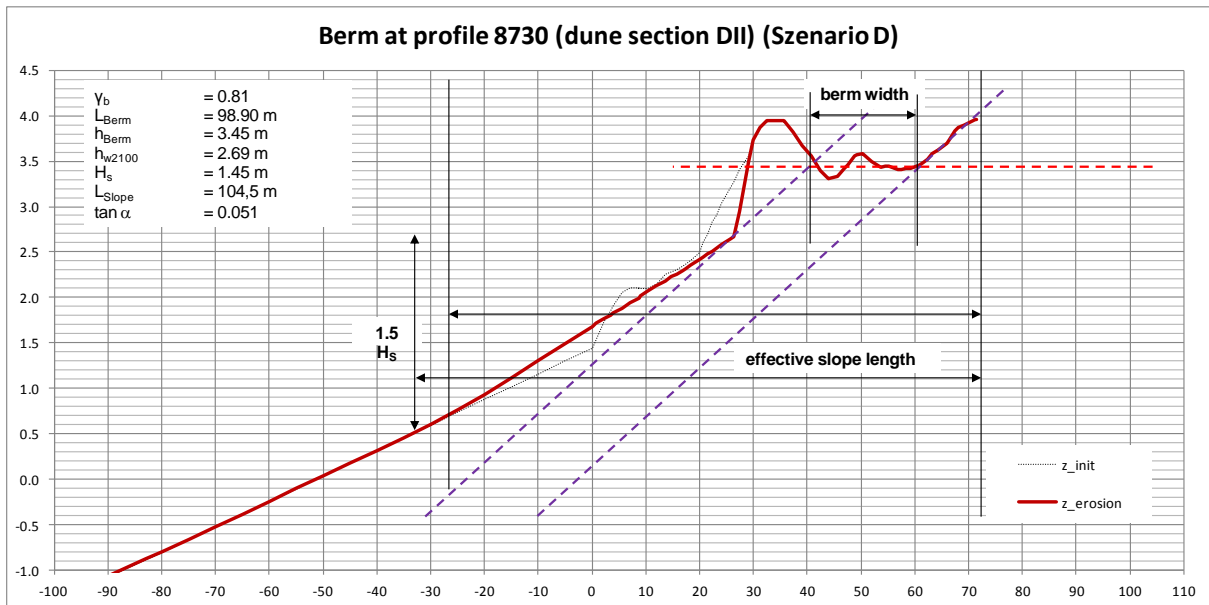


## Appendix B: Determination of the Berm Factor

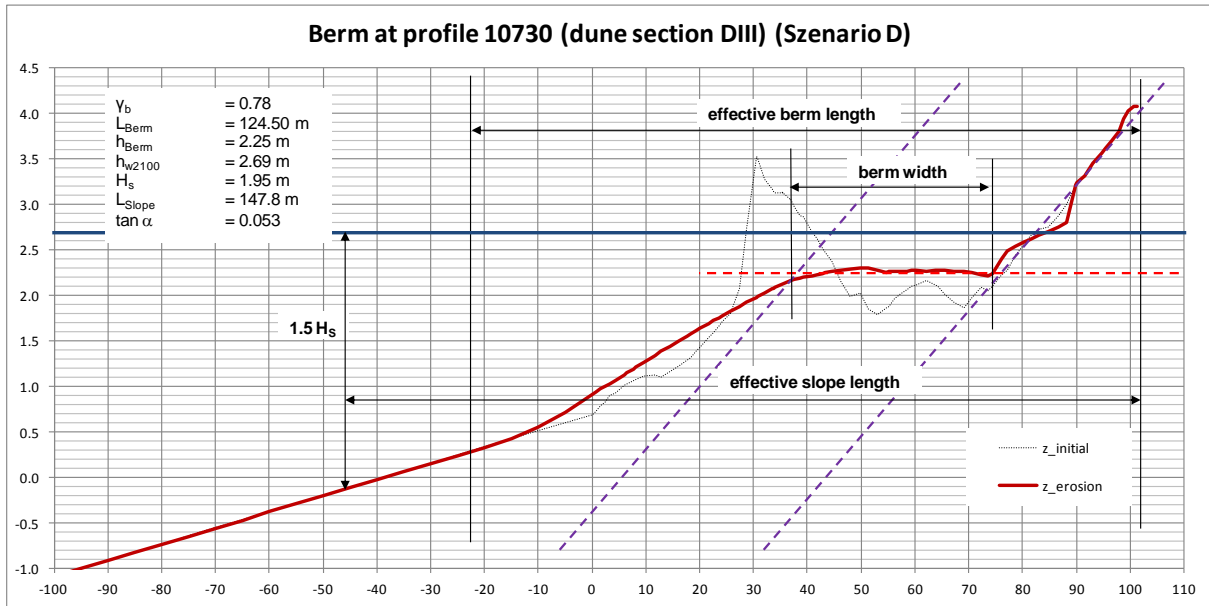
### Determination of the berm factor at dune section DI (Szenario D)



### Determination of the berm factor at dune section DII (Szenario D)

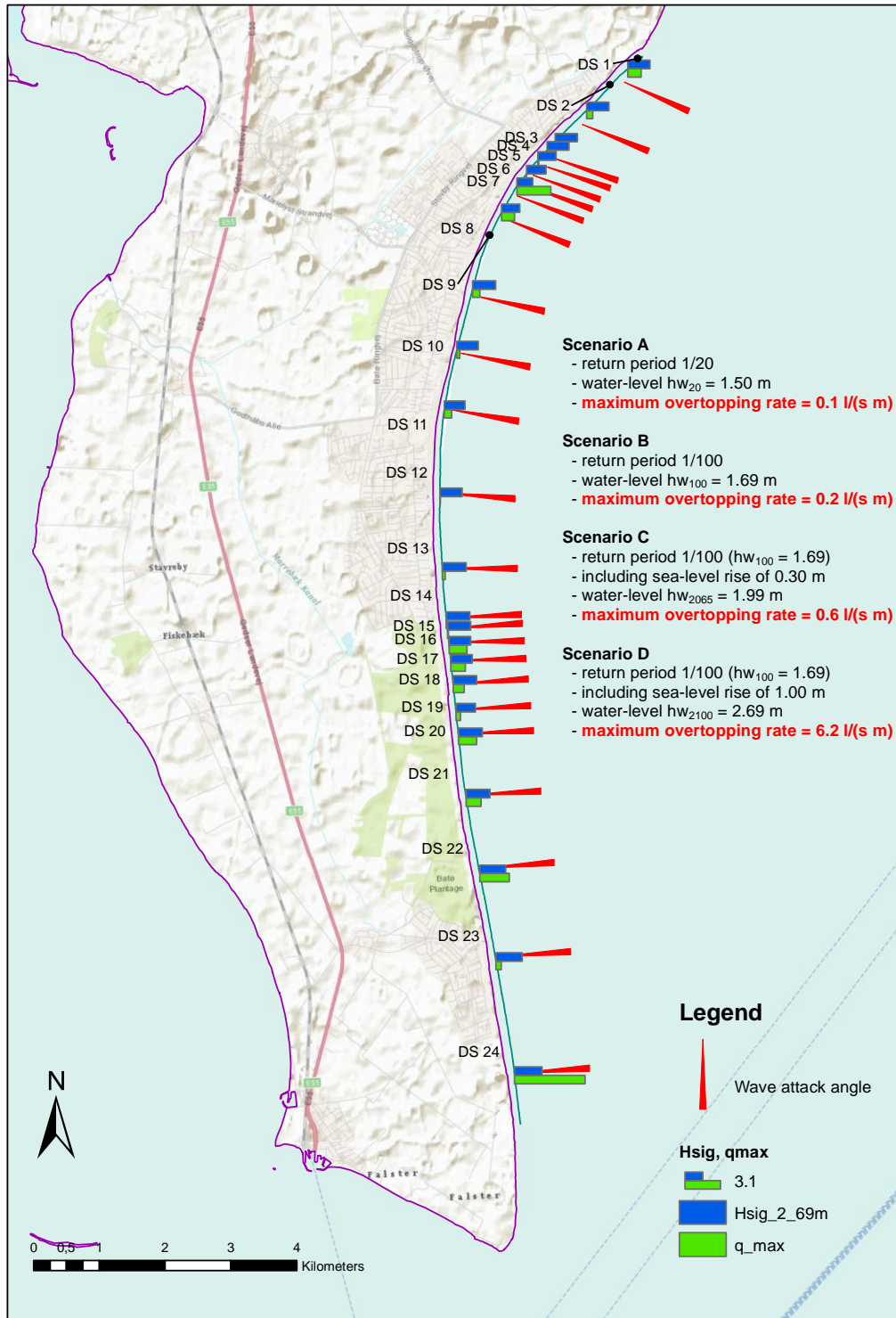


### Determination of the Berm Factor at Dune Section DIII



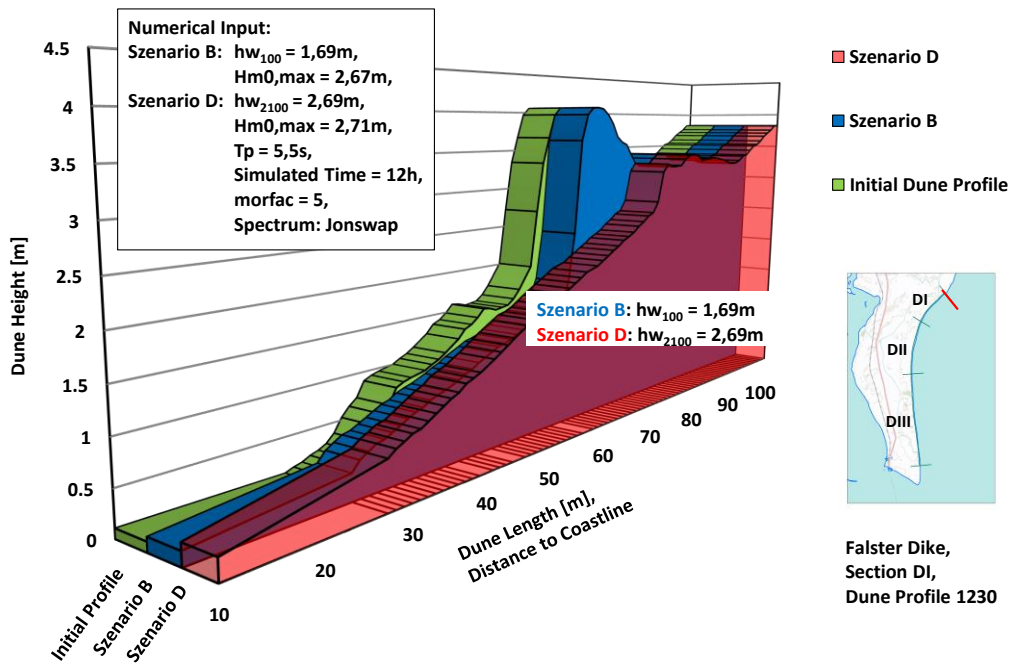
## Appendix C: Results of Sea State Simulation (SWAN)

**Scenario D: Wave height, wave attack angle and maximum overtopping rate in case of dike without considering dunes**

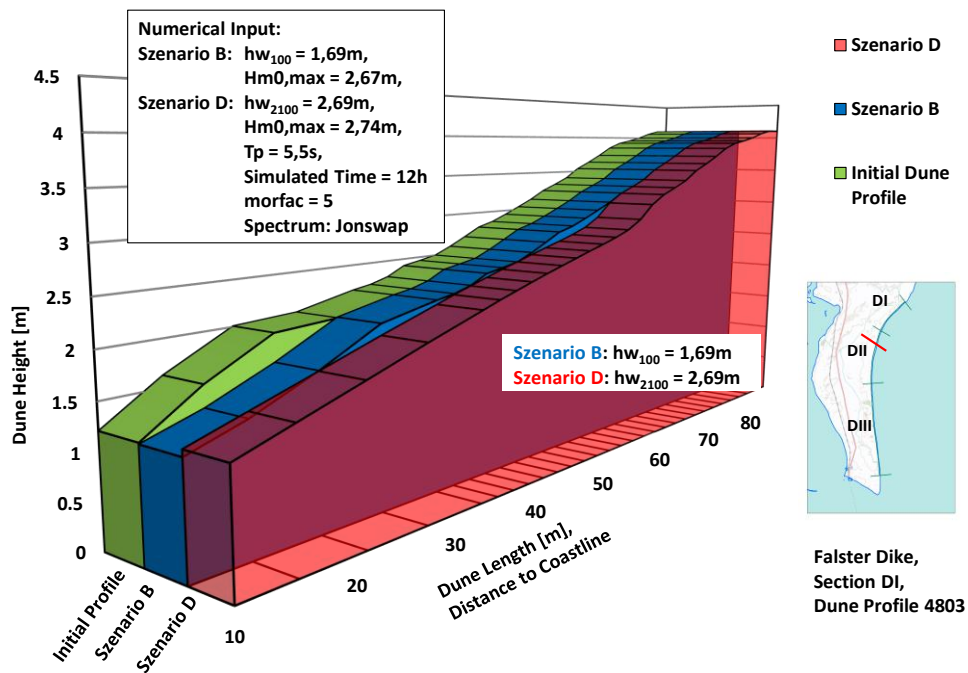


## Appendix D: Simulated Dune Erosion Cross Profiles

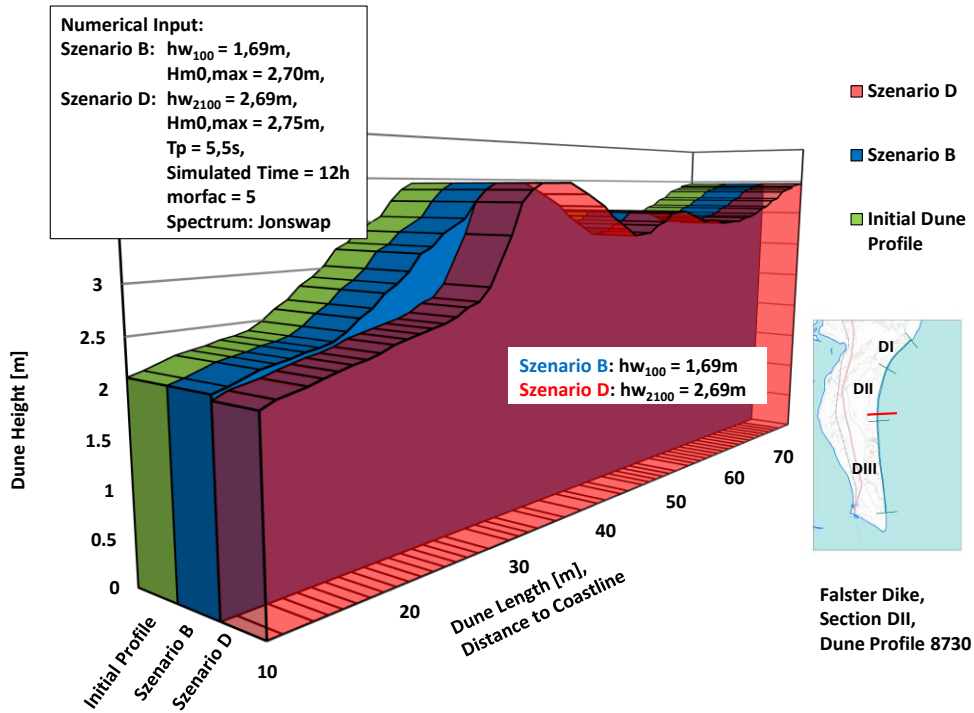
### 1. Erosion Profile (Dune Section DI, Profile 1230)



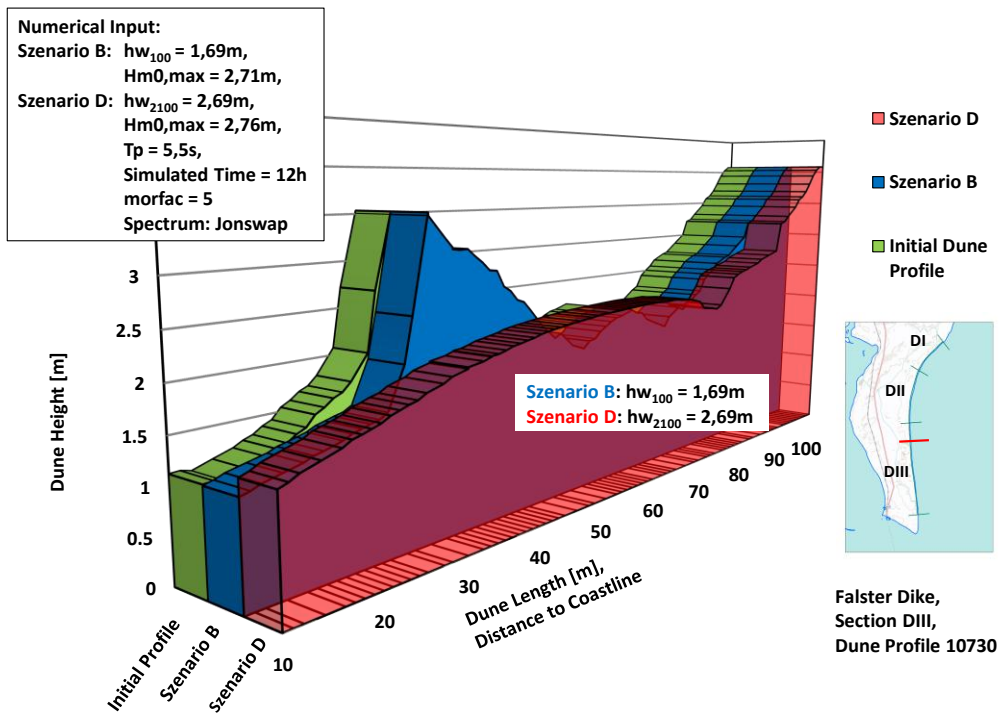
### 2. Erosion Profile (Dune Section DII, Profile 4803)



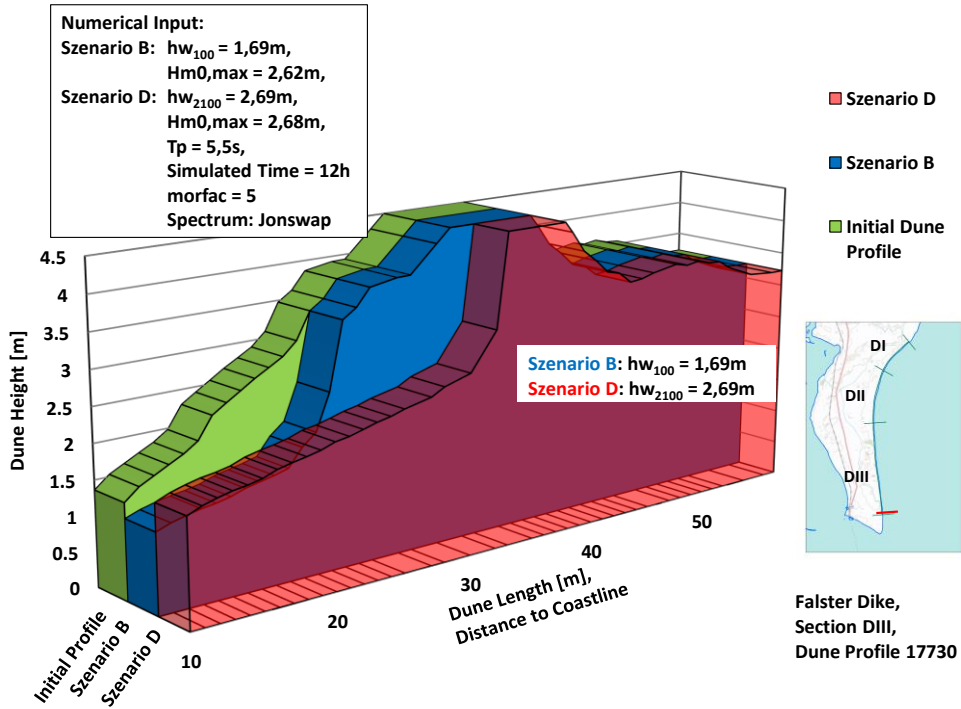
### 3. Erosion Profile (Dune Section DII, Profile 8730)



### 4. Erosion Profile (Dune Section DIII, Profile 10730)

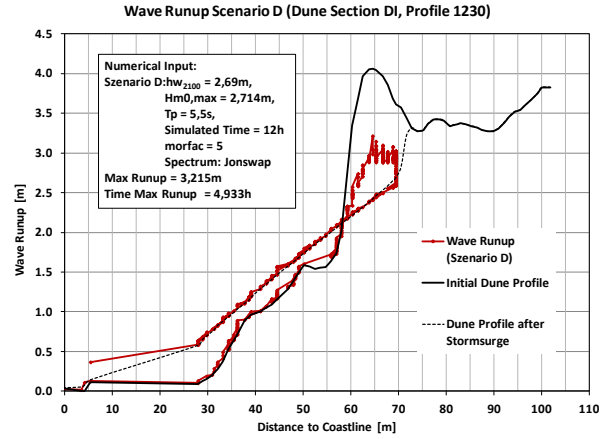
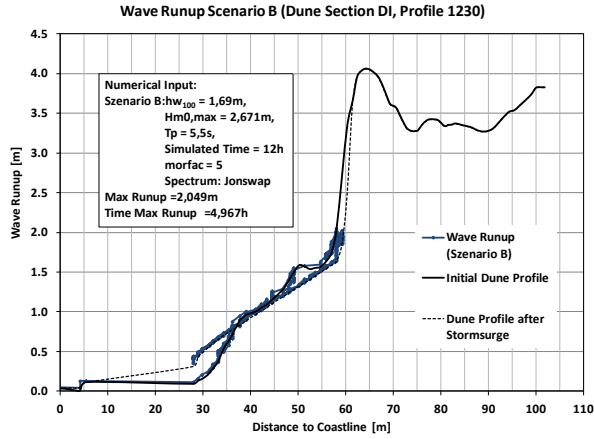


5. Erosion Profile (Dune Section DIII, Profile 17730)

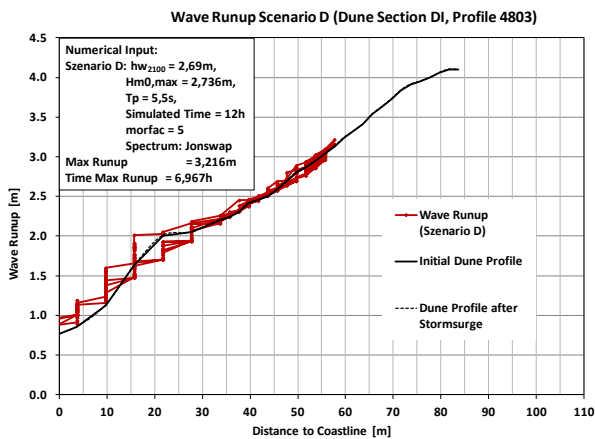
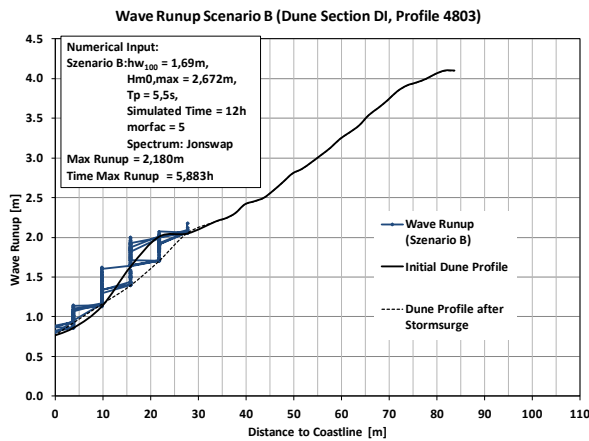


## Appendix E: Runup Level for Each Scenario

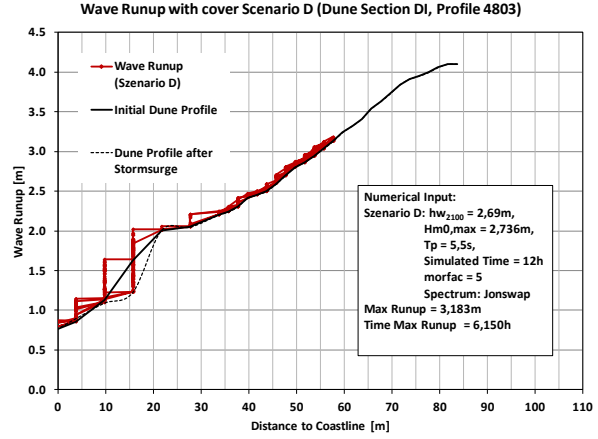
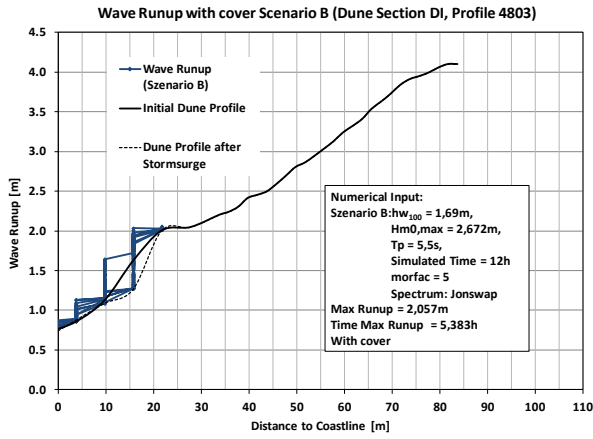
### 1. Profile 1230 wave runup



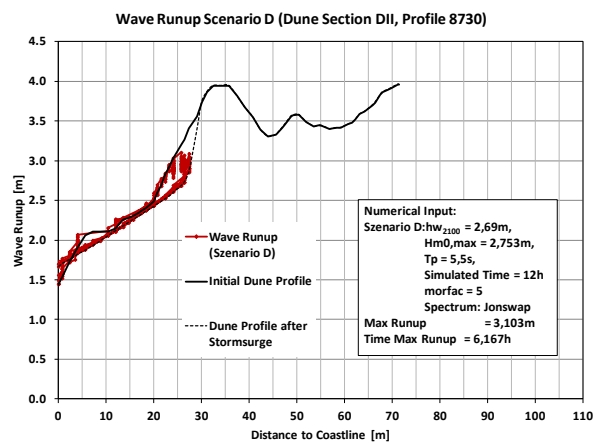
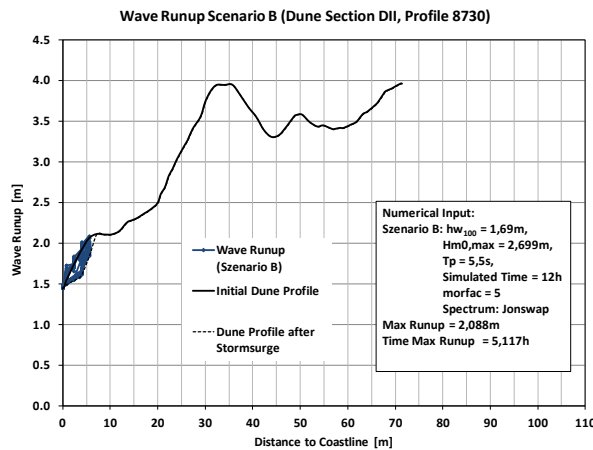
### 2. Profile 4802 wave runup



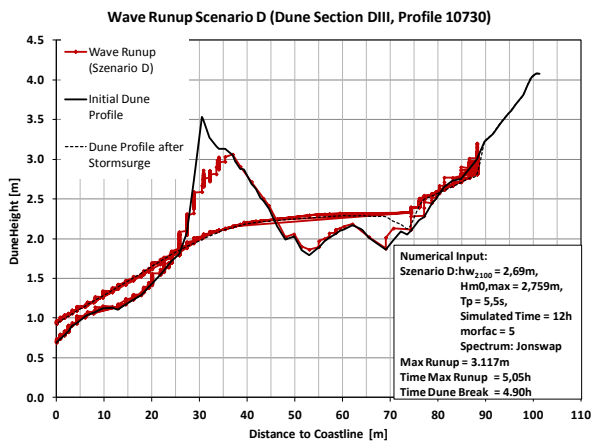
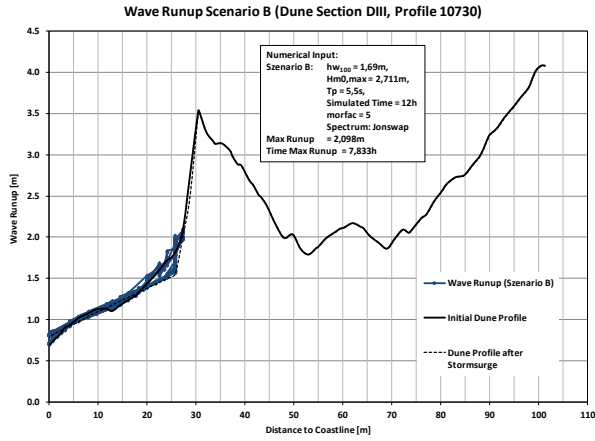
### 3. Profile 4803 with cover layer wave runup



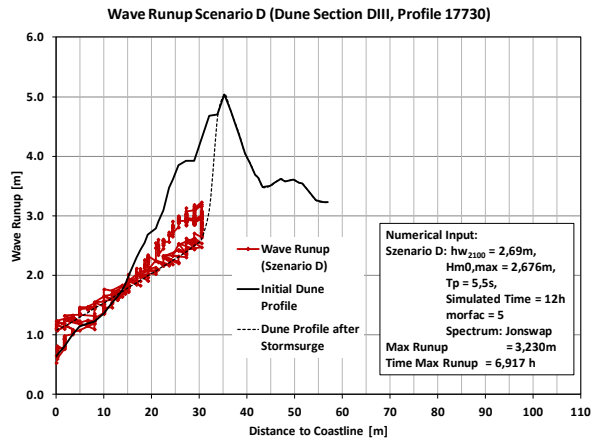
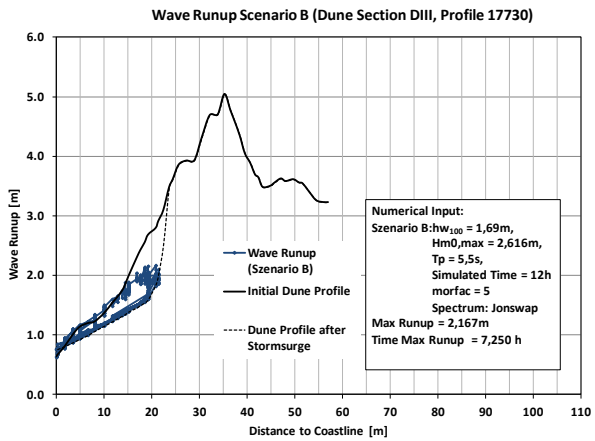
#### 4. Profile 8730 wave runup



#### 5. Profile 10730 wave runup



## 6. Profile 17730 wave runup



## Appendix F: Fault Tree of Probabilistic Approach

Fault tree with main failure mechanisms

